



The Chameleon Paradigm: An effective method for masking biological motion stimuli

Jiaxu Zhao^{1,2} · Xin He¹ · Yi Jiang^{1,2} · Min Bao^{1,2}

Received: 23 May 2025 / Accepted: 3 December 2025
© The Psychonomic Society, Inc. 2026

Abstract

Continuous flash suppression (CFS) is widely used in research on unconscious visual processing due to its long-lasting masking. While CFS effectively masks static stimuli, its application to motion stimuli remains challenging. To resolve this issue, our previous work developed the Chameleon-1 paradigm (Zhao & Bao, 2022), an enhanced CFS technique that enables robust masking of translational motion stimuli for up to 10 s through precise spatiotemporal matching of color dynamics between target and masking stimuli. The current study systematically evaluated and optimized this paradigm through three studies. We first assessed the masking efficacy of the Chameleon-1 paradigm across different motion parameters and patterns (Study 1). Because Chameleon-1 failed to effectively mask biological motion (BM) stimuli, we then upgraded the paradigm to accommodate BM stimulus characteristics (Study 2). The results demonstrated that this Chameleon-2 paradigm achieved superior masking efficacy for BM stimuli, with average breakthrough time extended by over two-fold compared to Chameleon-1 and breakthrough ratios approximately 75% for upright and 45% for inverted BM stimuli during 10-s of BM presentation. We further employed this paradigm to investigate the neural correlates of conscious and unconscious BM processing using functional near-infrared spectroscopy in Study 3. Our work establishes a robust paradigm for sustained masking of BM stimuli and validates its utility in unconscious processing research. We also provide new insights into the neural mechanisms underlying unconscious BM perception.

Keywords Biological motion · Continuous flash suppression · Unconscious processing · Motion

Introduction

Vision, our primary sense for interacting with the world, has a limited capacity. Although only a fraction of visual input reaches consciousness, substantial processing occurs unconsciously, supporting efficient interpretation of complex scenes. Key paradigms for studying unconscious processing include binocular rivalry, continuous flash suppression (CFS), and visual crowding (Kim & Blake, 2005).

Among these, CFS is particularly advantageous for investigating unconscious vision. It allows flexible stimulus placement and provides sustained, homogeneous suppression across large areas (Wang et al., 2022), making it ideal for studies requiring extended masking durations—such as those on unconscious priming or adaptation (Yang et al., 2014). In CFS, high-contrast Mondrian patterns shown to one eye suppress a static target presented to the other eye through interocular suppression (Faivre et al., 2014; Tsuchiya & Koch, 2005; Tsuchiya et al., 2006). While effective for static stimuli, CFS shows markedly reduced efficacy for motion stimuli (Pournaghdali & Schwartz, 2020; Wang et al., 2022).

Previous attempts to improve motion masking under CFS focused on enhancing motion congruence between target and mask (Pournaghdali & Schwartz, 2020). Moors et al. (2014) incorporated target motion parameters into their Moving Mondrian Mask, improving suppression for simple, single-point motion. Ananyev et al. (2017) extended this approach to more complex motion but still reported breakthrough in

✉ Yi Jiang
yijiang@psych.ac.cn

✉ Min Bao
baom@psych.ac.cn

¹ State Key Laboratory of Cognitive Science and Mental Health, Institute of Psychology, Chinese Academy of Sciences, 16 Lincui Road, Chaoyang District, Beijing 100101, China

² Department of Psychology, University of Chinese Academy of Sciences, Beijing 100049, China

over 70% of trials within 3 s. These efforts reveal two major limitations: reliance on motion matching alone remains insufficient, and effective masking of multi-point motion over prolonged durations has not been achieved.

To bridge the aforementioned research gaps, here we propose and systematically evaluate two novel paradigms named after a kind of animal, the chameleon. By dynamic color adaptation, chameleons are able to maintain perceptual congruence with their surroundings to avoid the risks of being detected by predators. Inspired by this natural phenomenon, we employed analogous camouflage principles to develop visual masking techniques capable of prolonged masking of multi-point/complex motion stimuli. This is achieved through continuous maintenance of perceptual congruence between elements of target and masking stimuli. Below we present the fundamental design principles underlying the two Chameleon paradigms.

The Chameleon-1 Paradigm: Sustained masking of translational motion

Our recently developed Chameleon-1 paradigm, designed to mask multi-point translational motion, significantly enhances the masking efficacy compared to conventional approaches (Zhao & Bao, 2022). This paradigm achieved superior masking performance (~25% breakthrough ratio) during extended 10-s presentations. Below, we detail the implementation protocol for this paradigm:

- **Eye-dominance test:** Under the classic CFS paradigm, one eye was presented with dynamic and chromatic Mondrian patterns, while the other eye with a static target (Dong et al., 2022; Zhao & Bao, 2022). The dominant eye was identified as the one showing higher breakthrough ratios during testing. Breakthrough ratio is the percentage of trials in which the target breaks into awareness.
- **Mask presentation (dominant eye):** No different from the classic CFS paradigm—dynamic and chromatic Mondrian patterns were presented to the dominant eye.
- **Target presentation (non-dominant eye):** The non-dominant eye viewed multi-point translational motion targets. A frame-by-frame alpha-blending technique dynamically matched target colors to corresponding mask regions.

The Chameleon-2 Paradigm: Dynamic masking of complex motion

Building upon the Chameleon-1 paradigm, we developed Chameleon-2, an advanced version specifically optimized for masking small, fast-moving complex stimuli. In the

current work, we focus on biological motion (BM) stimuli. Unlike the Chameleon-1 that manipulates the colors of target elements to match the corresponding regions of the Mondrian masks, this paradigm instead adopts random-dot masking stimuli and manipulates the locations of target elements to maintain strict color, size, and positional congruence between target and masking elements:

- **Eye-dominance test:** Identical to that of Chameleon-1.
- **Mask presentation (dominant eye):** Dynamic, multi-colored random-dot masking stimuli were presented to the dominant eye. Each masking dot was size-matched to a light-point element of the BM stimuli.
- **Target presentation (non-dominant eye):** The non-dominant eye viewed modified BM stimuli, with each light point dynamically repositioned via a frame-by-frame spatial alignment algorithm to maintain precise positional congruence with the most adjacent masking element in real time. The target and the spatially aligned masking elements also maintained color matching throughout presentation.
- While the current implementation focused on BM stimuli, the underlying methodological framework is inherently adaptable to any type of complex motion stimuli with appropriate parametric adjustments.

Compared to the motion-matching approaches, a critical advantage of the Chameleon paradigms is decoupling target and mask motion properties. This ensures that only targets carry coherent motion information, allowing independent manipulation of target motion while improving the masking efficacy for multi-point/complex motion. Although our prior work has demonstrated the feasibility of the Chameleon-1 paradigm (Zhao & Bao, 2022), two unresolved issues—parametric optimization and generalizability—limit its broader application. Therefore, this paper systematically investigated how motion speed, contrast, size, and motion pattern modulated masking efficacy (Study 1). Additionally, we developed the Chameleon-2 paradigm to specifically enhance masking effectiveness for complex motion patterns, particularly BM stimuli (Study 2). BM represents a distinct class of motion perception that involves coordinated displacement of multiple points representing an organism's articulations, simultaneously conveying both kinematic properties and socially meaningful information (Jiang & Wang, 2011; Johansson, 1973, 1976; Troje, 2013). Previous attempts to mask BM using the CFS paradigm yielded limited success (frequent breakthroughs at ≤ 2 s, Sun et al., 2017, 2022). If the Chameleon-2 paradigm proves effective in masking BM, it could serve as a powerful tool for investigating unconscious processing across diverse motion stimuli.

To assess the temporal limit of masking efficacy, we employed extended trial durations (10 s). Unlike many

breaking continuous flash suppression (b-CFS) studies, we prioritized breakthrough ratio over reaction time (RT). RT in b-CFS studies may originate from multiple processing stages rather than solely reflect unconscious processing alone, such as detection thresholds or expectation effects during transitional awareness states (Gayet et al., 2014; Stein et al., 2011), contamination from conscious processing (Sun et al., 2022), and non-perceptual factors like decision-making processes or response biases (Stein & Sterzer, 2014; Yang et al., 2014). Instead, the breakthrough ratio, calculated as the proportion of trials where target detection occurs, provides a more direct measure of masking efficacy, since trials with no response directly show that targets did not reach awareness threshold. In other words, this metric minimizes post-perceptual contamination while providing a clear binary awareness measure. Thus, we primarily used breakthrough ratio to evaluate masking efficacy, with RT as a secondary reference.

In Study 3, we applied the Chameleon-2 paradigm to examine the neural mechanisms underlying BM processing. Previous functional magnetic resonance imaging (fMRI, Allison et al., 2000; Deen et al., 2015; Pavlova & Sokolov, 2003) and transcranial magnetic stimulation (Troje, 2013) studies have identified the superior temporal sulcus (STS)—particularly the right STS (rSTS)—as a critical region of interest (ROI) for BM perception, which is also supported by recent functional near-infrared spectroscopy (fNIRS) work (Lisboa et al., 2020a, 2020b). Our Study 3 investigated neural correlates of Chameleon BM processing using fNIRS, demonstrating selective rSTS activation specifically during conscious, but not unconscious processing.

Study 1: The Chameleon-1 Paradigm

In Study 1, we evaluated the applicability of our proposed Chameleon-1 paradigm. Our investigations addressed four key parameters: (1) movement speed of target stimuli (Study 1a), (2) contrast relationships between masking and target stimuli (Study 1b), (3) size variations of both masking elements and targets (Study 1c), and (4) motion pattern, particularly for BM stimuli (Study 1d, see Section S2 of the supplementary information).

Study 1a: The influence of target speed on translational targets masking

In Study 1a, we investigated how target speed influenced masking effectiveness in the Chameleon-1 paradigm. We hypothesized that, as in the motion-matched CFS paradigm (Ananyev et al., 2017), masking efficacy would show an inverse relationship with target speed, with reduced masking at higher motion speeds.

Method

Participants We recruited 12 participants (six males and six females, $M_{\text{age}} = 23.67$ years, age range 19–26 years). The number of participants in Study 1 was predetermined based on the sample sizes from our previous work (Zhao & Bao, 2022). For all the present studies, participants were young volunteers from several universities in Beijing. They all had corrected-to-normal vision, with no history of color blindness or color deficiencies, and were naïve to the experimental hypotheses. They provided informed consent and received compensation upon completing the experiment. All experimental procedures were approved by the Institutional Review Board of the Institute of Psychology, Chinese Academy of Sciences.

Apparatus Stimuli were displayed on a 22-inch Dell E2213 monitor (1680 × 1050 resolution; 60-Hz refresh rate), calibrated using a Photo Research PR-655 spectrophotometer. Participants viewed the dichoptic stimuli through a mirror stereoscope at a viewing distance of 80 cm in a darkened room, with a chinrest to minimize head movements. The same equipment setup was used across all experiments in Study 1.

Stimuli All stimuli were generated using Psychtoolbox-3 (Brainard, 1997) in MATLAB (The MathWorks, Natick, MA, USA). A red central fixation point (RGB: [180 0 0]) was presented on a mid-gray background. Both masking and target stimuli were presented within a $10^\circ \times 10^\circ$ fusion box (see Fig. 1a), with each appearing on either the left or right half of the screen. The masking stimulus followed the same design as in our previous work (Zhao & Bao, 2022). We generated 60 Mondrian-pattern images ($8^\circ \times 8^\circ$), each consisting of randomly colored and sized rectangles. These images flickered at 10 Hz to serve as the CFS mask. The target stimulus comprised ten small squares ($1^\circ \times 1^\circ$) moving upward or downward at constant speed. Their positions were randomly selected within the $8^\circ \times 8^\circ$ area covered by the CFS stimulus, with the constraint of no inter-square overlap. While each square changed its position every one second, it maintained both its movement direction and speed. Crucially, in every frame, each square's color matched the corresponding pixels of the masking stimulus at that moment.

Based on previous findings showing successful 10-s masking at 0.2°/s in most trials (Zhao & Bao, 2022), we selected this as our baseline speed. To systematically examine speed effects, we additionally tested one slower (0.1°/s) and two faster (0.5°/s and 1°/s) speed conditions. Considering that motion-matched CFS research has shown ineffective masking efficacy at 1°/s (Ananyev et al., 2017), we constrained our speed conditions to no faster than 1°/s.

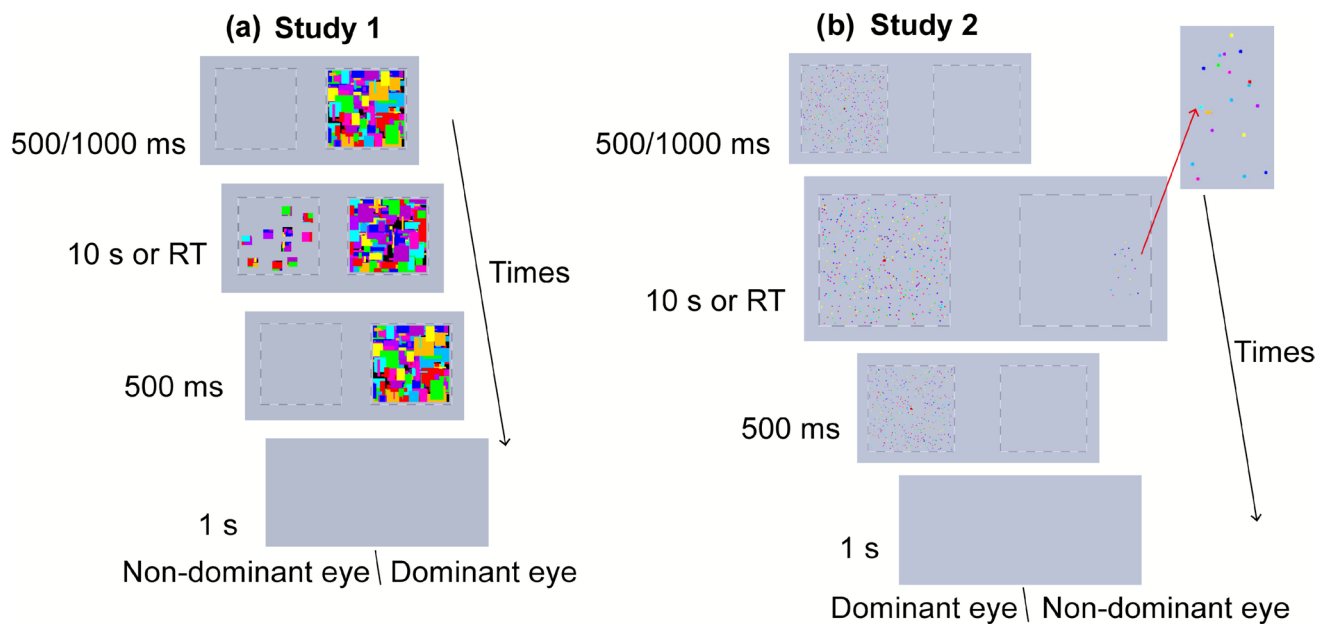


Fig. 1 The depiction of Study 1 and Study 2. *Note.* RT, reaction time. (a) A typical trial of Study 1. (b) The depiction of Study 2. The inset, magnified by the arrow, provides a detailed view of the target stimulus.

Procedure Participants first completed an eye-dominance test lasting approximately 10 min under the same experimental setup used in the formal experiments. The test employed identical stimuli and procedures to our previous work (Dong et al., 2022; Zhao & Bao 2022; see Figure S1, in Section S1 of the supplementary information), consisting of two blocks of 80 trials each.

During the formal experiment, we presented the masking stimulus to the dominant eye and the target stimulus to the non-dominant eye. The experiment comprised 12 blocks, each containing 16 trials (4 speed levels \times 4 repetitions), with equal numbers of upward and downward motions). Each trial (see Fig. 1a) began with a randomly determined CFS stimulus presentation (500 ms or 1000 ms) to the dominant eye. Subsequently, a target stimulus moving either upward or downward at one of the four speeds appeared in the non-dominant eye while the CFS mask continued in the dominant eye. Participants were instructed to indicate the target's moving direction as quickly as possible using arrow keys (UpArrow for upward, DownArrow for downward). If a key was pressed, the target immediately disappeared while the CFS mask persisted for an additional 500 ms. If no response was made, both stimuli automatically terminated after 10 s. Following the stimulus offset in either case, a 1-s inter-trial interval (mid-gray background) preceded the next trial. Throughout the experiment, both the masking and target stimuli maintained 100% contrast. Prior to the

formal experiment, participants completed 12 practice trials (three repetitions per speed level). The entire session lasted approximately 30 min.

Analysis For each participant, we calculated breakthrough ratios per speed condition by dividing the number of correct-response trials by the total trials for that condition ($n = 48$ per condition). A one-way repeated-measures ANOVA with speed (0.1°/s, 0.2°/s, 0.5°/s, 1°/s) as the within-subjects factor was conducted on breakthrough ratios.

Results

The descriptive results were presented in Table 1. As shown in Fig. 2a, we found a significant main effect of target speed ($F_{(1.671, 18.377)} = 36.724$, $p < 0.001$, $\eta^2_p = 0.770$, Greenhouse–Geisser corrected). Post hoc comparisons showed significantly lower breakthrough ratios at the slowest speed compared to the other speeds ($p_{\text{bonf}} \leq 0.009$, 95% CI $[-0.900, -0.039]$). The 0.2°/s condition also demonstrated lower breakthrough ratios than both 0.5°/s and 1°/s ($p_{\text{bonf}} \leq 0.002$, $[-0.705, -0.132]$), while no difference emerged between 0.5°/s and 1°/s ($p_{\text{bonf}} = 0.250$, $[-0.270, 0.044]$). The findings supported our hypothesis that faster target motion speeds would lead to increased breakthrough ratios, revealing the Chameleon-1's limited effectiveness for masking faster-moving stimuli.

Table 1 Means and standard errors of breakthrough ratios in Study 1a–c

Study 1a		Study 1b		Study 1c	
Target speed	Breakthrough ratio	Contrast pairing	Breakthrough ratio	Size pairing	Breakthrough ratio
0.1°/s	0.20 ± 0.05	1–0.1	0.26 ± 0.07	small-small	0.60 ± 0.09
0.2°/s	0.36 ± 0.06	1–0.5	0.35 ± 0.08	small-big	0.35 ± 0.09
0.5°/s	0.72 ± 0.09	1–1	0.38 ± 0.08	big-small	0.59 ± 0.09
1°/s	0.83 ± 0.07	0.5–0.5	0.44 ± 0.08	big-big	0.19 ± 0.07

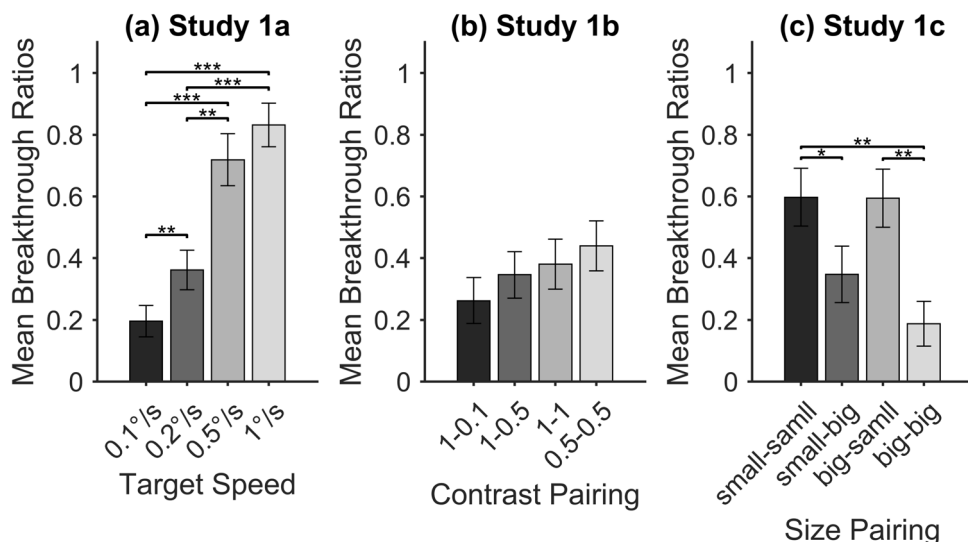


Fig. 2 Results for Study 1a–c. *Note.* Error bars represent ± 1 standard errors of means (SEM). Significance levels are indicated by asterisks: * $p < .05$, ** $p < .01$, *** $p < .001$. (a) Effects of target speed on translational target masking in Study 1a. (b) Masking efficacy across

four masking-target contrast pairing conditions in Study 1b. (c) Effects of four masking-target size pairing conditions on masking effects in Study 1c.

Study 1b: The influence of contrast pairing on translational target masking

Study 1b investigated how masking efficacy in Chameleon-1 was modulated by mask-target contrast relationships and whether the mechanisms involved in it were similar to those underlying the classic CFS paradigm. CFS is known to rely on the interocular suppression mechanisms, where high-contrast masks displayed in one eye suppress a target displayed in the opposite eye with target contrast incrementally ramped up (Cha et al., 2019; Jiang et al., 2007). By contrast, Chameleon-1 may involve a potential fusion-based mechanism due to its unique color consistency between masks and targets. We therefore tested two competing hypotheses: (1) If shared mechanisms operate in both paradigms, lower target contrast would enhance Chameleon-1’s masking efficacy as in the classic CFS paradigm. (2) If Chameleon-1 is actually driven by the binocular fusion mechanisms, then greater mask-target similarity (i.e., contrast consistency) would instead strengthen masking efficacy.

Method

Participants We recruited 12 new participants (six males and six females, $M_{age} = 24.25$ years, age range 20 to 29 years).

Stimuli The masking and target stimuli were identical to those in Study 1a except for the following changes. The target moved at a constant speed of 0.2°/s. Four mask-target contrast pairing conditions were used: [1, 0.1], [1, 0.5], [1, 1], [0.5, 0.5]. The first three contrast pairs would test whether the Chameleon-1 paradigm also exhibited stronger masking effects on the lower-contrast targets. The fourth matched-contrast condition tested whether this paradigm specifically relied on the binocular fusion mechanisms.

Procedure The experimental procedure matched that of Study 1a. Participants first completed an ocular-dominance test, followed by 12 practice trials before starting the formal experiment. In the formal experiment, the masking stimulus

was still presented to the dominant eye and the target stimulus to the non-dominant eye. The experiment consisted of 16 blocks (four blocks for each contrast combination), with the same contrast combination maintained throughout each block. The block presentation order was pseudo-randomized and counter-balanced across participants. Each block contained 12 trials. The trial structure and participant's task were identical to Study 1a, except for the different masking and target stimulus contrasts. The analysis method was the same as in Study 1a.

Results

The main effect of contrast combination reached significance ($F_{(1.708, 18.789)} = 4.560, p = 0.029, \eta^2_p = 0.293$, Greenhouse–Geisser corrected), yet none of the post-hoc pairwise comparisons with Bonferroni adjustment showed significant differences ($p_{\text{bonf}} \geq 0.162, [-0.400, 0.074]$, see Table 1 and Fig. 2b). Collectively, these findings demonstrate that varying contrast relationships between masking and target stimuli did not substantially alter the masking efficacy of the Chameleon-1 paradigm. This contrast-invariant masking efficacy suggests a distinct mechanistic basis that differs from the contrast-dependent suppression characteristic of the CFS paradigm.

Study 1c: The influence of size pairing on translational target masking

Study 1c examined how target size modulated masking efficacy in the Chameleon-1 paradigm. Because the masking effect in this paradigm presumably relied on the induced perceptual fusion between mask and target stimuli, we hypothesized that increasing target size would cause stronger binocular fusion, which consequently augmented the masking effect.

Method

Participants Twelve participants (five males and seven females, $M_{\text{age}} = 22.00$ years, age range 19 to 27 years) participated in Study 1c.

Stimuli The moving speed of target stimulus was fixed at 0.2°/s, and the target contrast remained constant at 1. The target stimulus was rendered in the same way as in Studies 1a and 1b, with the color of each target square matching the color of the corresponding pixels of the masking stimulus in each frame. Unlike previous studies that employ size-matched mask and target elements (typically approximately 0.5° visual angle; Ananyev et al., 2017; Moors et al., 2014), we implemented a 2 × 2 factorial design with mask sizes (0.5°, 1°) and target sizes (0.5°, 1°) to create four distinct

size-pairing conditions: small-small, small-big, big-small, and big-big. This design specifically tested our hypothesis that larger target stimuli would enhance the masking efficacy in the Chameleon-1 paradigm. Thus, we modified the number of the masking elements to ensure that the masking elements could fill the 8° × 8° masking region. Specifically, the masking stimulus consisted of either 580 squares (0.5°, smaller elements) or 250 squares (1°, bigger elements).

Procedure The experimental procedure followed Study 1a with the following modifications: there were a total of eight blocks, each containing 24 trials. Within each block, the masking element size remained constant (counter-balanced across blocks), while the target size varied between 0.5° (half of trials) and 1° (remaining trials). These two trial types were pseudo-randomly interleaved within each block. The analysis method matched that of Study 1a.

Results

Our analysis showed a strong main effect of size combination ($F_{(3, 33)} = 13.998, p < 0.001, \eta^2_p = 0.560$). Post-hoc comparisons of size conditions demonstrated significantly higher breakthrough ratios in the small-small condition compared to both the small-big and big-big conditions ($p_{\text{bonf}} \leq 0.046, [0.003, 0.706]$). Similarly, the big-small condition showed elevated breakthrough ratios relative to the big-big ($p_{\text{bonf}} = 0.005, [0.119, 0.693]$). These suggested that the Chameleon-1 paradigm's masking efficacy primarily depended on the target size rather than the masking element dimensions, with optimal performance occurring when targets were relatively large (see Table 1 and Fig. 2c), thereby confirming our original hypothesis.

Study 1d: An attempt to mask BM targets using Chameleon-1

In Study 1d, we investigated the efficacy of the Chameleon-1 paradigm in masking complex motion patterns, specifically BM stimuli (see Section S2 of the supplementary information). The findings demonstrated that the Chameleon-1 paradigm failed to effectively mask the BM stimuli. The breakthrough ratios approached ceiling levels (near 100%), while the median RTs consistently averaged approximately 2 s across participants (see Figure S3 in Section S2 of the supplementary information).

Interim discussion

Study 1 examined the masking efficacy of the Chameleon-1 paradigm through four critical parameters: motion speed, contrast, size, and motion pattern. Our results demonstrated that the Chameleon-1 paradigm exhibited

stronger masking efficacy for slow-moving, large target stimuli. However, variations in contrast between the mask and target stimuli did not yield statistically significant differences in masking performance. Notably, the paradigm proved ineffective in masking BM stimuli.

Previous findings have shown that faster target motion (e.g., 1°/s) significantly reduced masking effectiveness (Ananyev et al., 2017; Hong & Blake, 2009). Similarly, our Chameleon-1 paradigm failed to effectively mask targets moving at 1°/s, suggesting a fundamental limitation in applying these paradigms for studying unconscious motion processing. Importantly, Chameleon-1 shows contrast-independent masking mechanism. It is well known that classic CFS paradigms exploit interocular suppression mechanisms to mask targets. To extend masking duration, researchers often present the target stimulus in a gradual fade-in (ramping up its contrast) manner (e.g., del Río et al., 2018; Liu et al., 2016; Mudrik et al., 2011; Sun et al., 2022), then maintaining CFS stimuli at high contrast to ensure robust masking (e.g., Dong et al., 2022; Han et al., 2016, 2019; Ludwig et al., 2016). By contrast, the Chameleon-1 paradigm relies on consistent target-mask colors and positions, suggesting that this approach involves fundamentally different masking processes based on binocular fusion rather than interocular competition. Accordingly, high-contrast targets promote stable fusion through strong color consistency with masks, while low-contrast targets, despite their reduced salience, simultaneously exhibit diminished color consistency that disrupts fusion stability. These opposing influences ultimately produce comparable masking efficacy across contrast conditions. Moreover, we found superior masking for larger target stimuli, which we attribute to enhanced pattern matching between the extended spatial configuration of the larger stimuli and the masking pattern, thereby facilitating binocular fusion.

However, the light points of typical BM stimuli are often small (e.g., 0.1°) and moving at relatively higher speed (> 1°/s, particularly for the feet points). Therefore, the masking efficacy of Chameleon-1 for BM stimuli was unsatisfactory. To address these constraints, we implemented targeted modifications in Study 2.

Study 2: The Chameleon-2 Paradigm

We developed an enhanced Chameleon-2 paradigm in Study 2. This new paradigm adopts random-dot masks and enforces strict size, color and spatial alignment between target stimuli and masking elements, ensuring their real-time perceptual correspondence (for details see Stimuli section of Study 2a).

Study 2a: Masking of BM targets using Chameleon-2

In Study 2a, we pursued two key objectives: (1) developing the Chameleon-2 paradigm to specifically accommodate the distinctive characteristics of BM stimuli, and (2) investigating how target-mask color consistency influences masking efficacy.

Method

Participants Twenty participants (seven males and 13 females, $M_{\text{age}} = 21.70$ years, age range 18–25 years) participated in Study 2a. The numbers of participants in Study 2 were predetermined based on the sample sizes of recent b-CFS studies on BM (Sun et al., 2017, 2022).

Stimuli A red central fixation point (RGB: [255 0 0]) was presented on a mid-gray background of the screen. To facilitate binocular fusion, two 10° × 10° fusion frames were presented on the left and right screen halves. The masking stimulus consisted of solid-colored circular elements in ten distinct colors (RGB values: [255 0 0], [255 255 0], [0 255 0], [0 0 255], [255 0 128], [0 255 255], [255 128 0], [128 0 255], [0 128 255], [128 0 128]). We generated 95 stimulus images (each subtending 9.96° × 9.96°) containing 500 masking elements (0.1° diameter, five elements/deg² density), with randomized colors and positions. All elements flickered at 60 Hz.

The BM target was generated using PsychToolbox-3 (Brainard, 1997) and BioMotion Toolbox (van Boxtel & Lu, 2013) in MATLAB (The MathWorks, Natick, MA, USA), adopting the same motion-capture source (Carnegie Mellon Graphics Lab Motion Capture Database: <http://mocap.cs.cmu.edu>, document number: 08_04.c3d) and processing pipeline as Mei et al. (2018). Following Mei et al.'s (2018) protocol, we selected 20 of the original 41 light points to construct the point-light walker (PLW), and extracted one walking cycle (frames 235–329) for stimulus generation. Therefore, a total of 95 frames of images were created with 60-Hz position updates for the light points. Each light point had a diameter of 0.1°, matching the size of the masking stimulus elements, while the complete BM stimulus subtended 2.4° × 3.2°. Using the BioMotion Toolbox, we applied four modifications to the original upright, rightward-walking BM stimulus derived from the motion capture data. All the BM stimuli were pre-generated offline through the following steps: (1) applying the Smooth function to ensure smooth transitions between walking cycles; (2) translating the BM stimulus 2.74° leftward or rightward for visual field positioning; (3) rotating the rightward-walking stimulus 180° to create leftward-walking versions; and (4) using the Invert function to generate inverted variants from both upright leftward- and

rightward-walking stimuli. This procedure yielded eight final stimulus types: left-visual-field leftward-upright (LVF-LU), left-visual-field rightward-upright (LVF-RU), left-visual-field leftward-inverted (LVF-LI), LVF-RI, RVF-LU, RVF-RU, RVF-LI, and RVF-RI. To strengthen the masking effect, we modified the original 20 light point positions (output from BioMotion Toolbox) by aligning each point with the nearest circular element in the corresponding masking stimulus frame. This process created 95 stimulus pairs (one target and one masking image per frame). For each pair of stimuli, we identified the 20 masking elements closest to the original light point positions, and used these element positions as the actual light point locations (see Fig. 3c). If multiple light points happened to have the same nearest circular element, duplicate assignments were resolved by selecting progressively distant elements (second-nearest, etc.). This guaranteed exactly 20 distinct light points per frame. The resulting positional offset measured $0.22^\circ \pm 0.02^\circ$ (mean \pm SD), representing 29.73% of the average skeleton length ($0.74^\circ \pm 0.53^\circ$). Consequently, the signal-to-noise ratio of BM information was calculated as 70.27% (1 - offset percentage). We call this target stimulus Chameleon BM. By using the upright/inverted BM stimuli, we also examined whether our Chameleon targets preserved BM information or not through the well-established inversion effects (i.e., higher breakthrough ratios for the upright versus inverted BM stimuli, Sun et al., 2022).

After determining the positions of the 20 light points, we implemented three target stimulus conditions based on color consistency with the masking stimulus. In the color-consistent condition, the 20 light points in the target stimulus

adopted both the positions and colors of their corresponding masking stimulus elements. For the color-inconsistent condition, each light point's color was randomly selected from the ten colors comprising the masking stimulus, maintaining positional matching but varying colors. The black condition preserved the same positional matching while rendering all light points black. Crucially, while light point positions remained consistent with masking elements across all three conditions, color consistency served as our independent variable. This design yielded 24 stimulus groups (8 types \times 3 conditions), with each group containing 95 target images systematically paired with 95 masking stimuli.

Procedure The formal experiment comprised eight blocks, with each block containing 24 trials (8 stimulus types \times 3 conditions). Each trial began with the masking stimulus presented alone to the dominant eye for either 500 or 1000 ms. Subsequently, while the masking stimulus continued, a target stimulus appeared in the non-dominant eye. Participants were instructed to indicate the PLW's walking direction immediately upon detection using the corresponding key press (LeftArrow for leftward, and RightArrow for rightward). Only correct responses were counted as breakthroughs. Upon key press, the target stimulus disappeared while the masking stimulus persisted for an additional 500 ms. If no response was made within 10 s, both stimuli terminated simultaneously. During simultaneous presentation of the masking and target stimuli, the pre-generated stimulus pairs were displayed in a continuous loop (95 frames/loop, \sim 1.6 s per loop). Following stimulus offset (regardless of participant response), a 1-s inter-trial interval

(a) Original BM (b) Stimulus Comparison (c) Chameleon BM (d) Position-Inconsistent BM

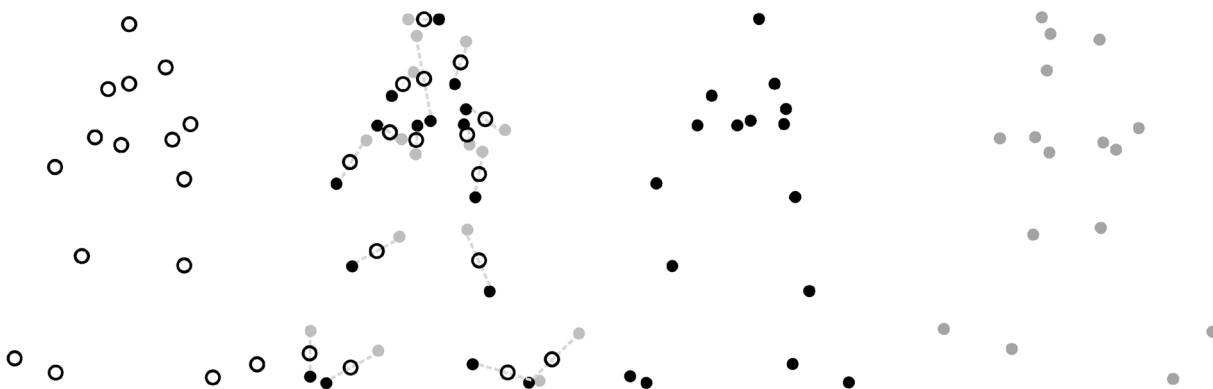


Fig. 3 Schematic illustration of target stimuli generation in Study 2. *Note.* (a) Original BM stimulus generated by BioMotion Toolbox. (b) *Black open circles* (identical to panel a) show theoretical positions from the BioMotion Toolbox. *Black solid circles* show the target positions for Study 2a, aligned with the positions of their nearest masking stimulus elements. *Mid-gray solid circles* show the target positions for the position-inconsistent condition in Study 2b (mirror-

symmetric the *black solid circles* across the *open circles*). The *dashed lines* are used to clarify their mirror-symmetric relationship. (c) The Chameleon BM stimulus for Study 2a and the position-consistent condition in Study 2b. (d) The Chameleon BM stimulus for the position-inconsistent condition in Study 2b. While we actually used 20-light-point stimuli in the studies, this schematic displays only 16 light points for better visualization purpose.

(mid-gray background) preceded the next trial (see Fig. 1b). Both the masking and target stimuli maintained 100% contrast throughout the experiment. Between blocks, an on-screen message ("Take a break! You still have N blocks to complete. Press 'space' to continue.") allowed participants to rest briefly before proceeding to the next block via spacebar press. Prior to the formal experiment, participants completed 12 practice trials to acclimate to the task. The formal experiment duration was approximately 35 min.

Additionally, in the Chameleon-2 paradigm, all light point positions in each target stimulus frame are derived from the masking stimulus, which means that the positional information is embedded within the masking stimulus. To verify participants could not utilize this embedded information, we conducted a control experiment following the main task (see Section S3 of the supplementary information for details).

Analysis We performed a repeated measures ANOVA with two within-subject factors: target condition (color-consistent, color-inconsistent, black) and target orientation (upright, inverted). The analysis included two dependent measures: mean breakthrough ratios and median RTs. For RT calculations, we considered only correct-response trials and non-response trials, with non-responses coded as the maximum stimulus duration (10 s).

Table 2 Means and standard errors of breakthrough ratios in Study 2a

Condition	Overall	Upright	Inverted
Color-consistent	0.69 (0.04)	0.87 (0.02)	0.52 (0.07)
Color-inconsistent	0.63 (0.06)	0.78 (0.06)	0.48 (0.07)
Black	0.88 (0.02)	0.99 (0.01)	0.77 (0.04)

Table 3 ANOVA and post hoc comparisons for breakthrough ratios in Study 2a

Main effects and interaction	F-value	df	p value	η^2_p
Condition (main effect)	19.544	1,449, 27,524	< 0.001	0.507
Orientation (main effect)	54.558	1, 19	< 0.001	0.742
Condition × orientation	6.386	2, 38	0.004	0.252
Post hoc comparisons		p_{bonf}	95% CI	
Color-consistent vs. color-inconsistent		0.423	[- 0.043, 0.163]	
Color-consistent vs. black		< 0.001	[- 0.265, - 0.109]	
Color-inconsistent vs. black		< 0.001	[- 0.383, - 0.111]	
Main effect contrast		p value	95% CI	
Upright vs. inverted		< 0.001	[0.207, 0.370]	

The *df* for the main effect of condition are Greenhouse–Geisser corrected. p_{bonf} = Bonferroni-corrected *p* value. CI = confidence interval.

Results

For the trials where the BM target reached awareness, participants accurately reported its walking direction (92.11% ± 1.73%). Descriptive statistics and ANOVA results are presented in Tables 2 and 3, respectively. Regarding the breakthrough ratios, a significant main effect of target condition was found. Specifically, the breakthrough ratios in the color-consistent condition and color-inconsistent condition were significantly lower than that in the black condition. No significant difference was observed between the color-consistent and color-inconsistent conditions. These results suggested that the masking effect was more effective when the BM target shared color properties with the masking stimulus, regardless of whether their colors matched. Moreover, a significant main effect of target orientation was observed, with the upright targets exhibiting a higher breakthrough ratios compared to the inverted targets. This inversion effect aligns with the prior findings demonstrating that BM stimuli are sensitive to orientation (Troje & Westhoff, 2006), confirming that the Chameleon BM target maintained its BM properties.

A significant two-way interaction between the target condition and orientation was also found (see Fig. 4a). First, a robust inversion effect occurred across all the target conditions ($p_{\text{bonf}} < 0.001$, [0.130, 0.448]). Specifically, the inversion effect was stronger in the color-consistent condition than in the black condition ($p_{\text{bonf}} = 0.001$, [0.051, 0.209]). Additionally, within each BM orientation, both the color-consistent and color-inconsistent conditions showed lower breakthrough ratios than the black condition ($p_{\text{bonf}} \leq 0.006$, [- 0.433, - 0.055]). Further analysis revealed that the disparity in breakthrough ratios between the color-consistent and black conditions was larger for the inverted versus upright targets ($p_{\text{bonf}} < 0.001$, [- 0.193, - 0.067]).

The RT results exhibited a similar pattern. For the reasons outlined in the Introduction, we only present the grand median and individual data in Fig. 4b, omitting formal

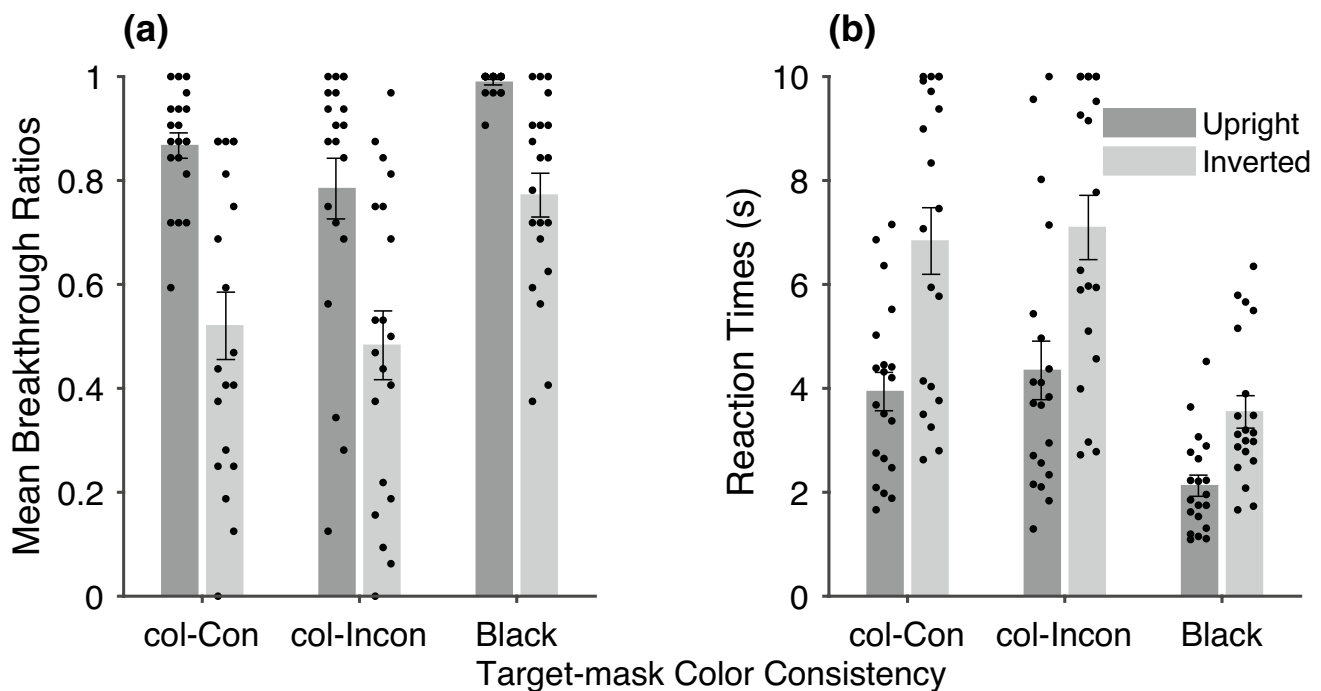


Fig. 4 Results for Study 2a. *Note.* Error bars represent ± 1 SEM. col-Con, color-consistent condition; col-Incon, color-inconsistent condition. The dots show the individual data. The results of (a) breakthrough ratios and (b) median RTs across target-mask color consistency in Study 2a.

statistical reporting. A supplementary analysis was conducted to examine the proportion of non-response trials. Non-response trials were defined as those in which no target detection occurred throughout the entire 10-s presentation window. Critically, the pattern of results for the non-response trials mirrored that of the breakthrough ratios (see Table S1 and Figure S5a, in Section S4 of the supplementary information). This measure provides a complementary assessment of full masking efficacy, augmenting insights from breakthrough ratio analyses. Furthermore, the control experiment revealed that the masking stimulus contained no coherent motion information that could be either consciously detected or reliably reported (see Figure S4, in Section S3 of the supplementary information).

Study 2b: The role of position consistency

Study 2a examined how target-mask color consistency affected the masking efficacy of Chameleon-2. Study 2b further tested the necessity of target-mask positional consistency for successful masking within this paradigm. For this goal, we included a position-inconsistent (control) condition to compare it with the position-consistent condition. The spatial offset of each light point relative to its corresponding original BM element was kept comparable across the two conditions, yet only the light points in the position-consistent condition aligned with the masking elements. Therefore, any observed advance of the masking

efficacy of the position-consistent condition relative to the position-inconsistent condition would reflect the expected role of spatial correspondence in masking.

Method

Participants We recruited 20 participants (seven males and 13 females, $M_{\text{age}} = 23.10$ years, age range 18–27 years) in Study 2b.

Stimuli Similar to Study 2a, we used eight types of target stimuli flickering at 60 Hz, but defined conditions by position consistency rather than color consistency. Three position-determination methods were employed: (1) position-consistent condition (analogous to Study 2a's color-inconsistent condition) where each light point's position matched its nearest masking element while its color was randomly selected from the ten masking stimulus colors (see Fig. 3c); (2) position-inconsistent condition (same color assignment as position-consistent) where each light point's position was determined by mirroring its position-consistent location across its BioMotion-calculated position (see Fig. 3d), maintaining equal distance from the calculated position while differing from masking elements; and (3) black condition (all black light points). We split trials in the black condition equally between the position-consistent and position-inconsistent determination methods to prevent

learning bias from unequal supra-threshold PLW exposures during breakthroughs.

Procedure The experimental procedure and task were similar to Study 2a. The data analysis followed the same approach as in Study 2a.

Results

Participants demonstrated competent performance in judging the walking direction of the BM target (88.72% ± 1.61%). Descriptive statistics and ANOVA results are presented in Tables 4 and 5, respectively. The ANOVA on breakthrough ratios revealed a significant main effect of target condition. The position-consistent condition yielded significantly lower breakthrough ratios than both the position-inconsistent and black conditions. Additionally, the position-inconsistent condition showed significantly lower breakthrough ratios than the black condition. These results replicate the finding in Study 2a that the black BM targets broke into awareness more easily than the colorful ones when using colorful masking stimuli. More importantly, the results indicate that the position consistency between the BM target and mask substantially strengthens the masking effectiveness. We also found a main effect of target orientation, showing higher breakthrough ratios for the upright targets compared to the inverted ones. This replicates the characteristic inversion effect in BM processing.

Table 4 Means and standard errors of breakthrough ratios in Study 2b

Condition	Overall	Upright	Inverted
Position-consistent	0.53 (0.06)	0.66 (0.06)	0.39 (0.06)
Position-inconsistent	0.69 (0.05)	0.81 (0.05)	0.56 (0.05)
Black	0.89 (0.02)	0.98 (0.01)	0.80 (0.04)

Table 5 ANOVA and post hoc comparisons for breakthrough ratios in Study 2b

Main effects and interaction	F-value	df	p value	η^2_p
Condition (main effect)	26.101	1,453, 27,605	< 0.001	0.579
Orientation (main effect)	53.887	1, 19	< 0.001	0.739
Condition × orientation	3.833	2, 38	0.030	0.168
Post hoc comparisons	p_{bonf}		95% CI	
Position-consistent vs. position-inconsistent	0.001		[- 0.257, - 0.066]	
Position-consistent vs. black	< 0.001		[- 0.529, - 0.198]	
Position-inconsistent vs. black	0.001		[- 0.328, - 0.075]	
Main effect contrast	p value		95% CI	
Upright vs. inverted	< 0.001		[0.169, 0.305]	

The *df* for the main effect of condition are Greenhouse–Geisser corrected. p_{bonf} = Bonferroni-corrected *p* value. CI = confidence interval.

Besides, the interaction between the target condition and orientation was significant (see Fig. 5a). Notably, significant inversion effects were present across all target conditions ($p_{\text{bonf}} \leq 0.001$, [0.114, 0.342]). Post hoc comparisons showed stronger inversion effects in the position-consistent condition than in the black condition ($p_{\text{bonf}} = 0.028$, [0.007, 0.158]). Within each BM orientation, the position-consistent condition showed lower breakthrough ratios than the position-inconsistent condition, with both being lower than the black condition ($p_{\text{bonf}} \leq 0.019$, [- 0.578, - 0.024]). The interaction manifested as a larger difference in breakthrough ratios between the position-consistent and black conditions for the inverted versus upright targets ($p_{\text{bonf}} = 0.009$, [- 0.143, - 0.022]).

The RT results, showing patterns similar to the breakthrough ratios, are presented in Fig. 5b without statistical reporting to maintain the focus on the primary findings. A similar pattern was also observed in the proportion of non-response trials (see Table S2 and Figure S5b, in Section S4 of the supplementary information).

Study 2c: Binocular fusion of Chameleon-2

To investigate the underlying mechanisms of the Chameleon-2 paradigm, Study 2c employed binocular eye-tracking, testing whether the target’s breakthrough stems from imperfect fusion led by fixation disparity (Ogle et al., 1949) rather than unconscious BM processing (see Section S5 of the supplementary information). Crucially, our analyses revealed no significant differences in the fixation disparity between the breakthrough and non-response trials, suggesting stable binocular fusion during the BM observation and eliminating fusion disruption as a potential mechanism for breakthrough.

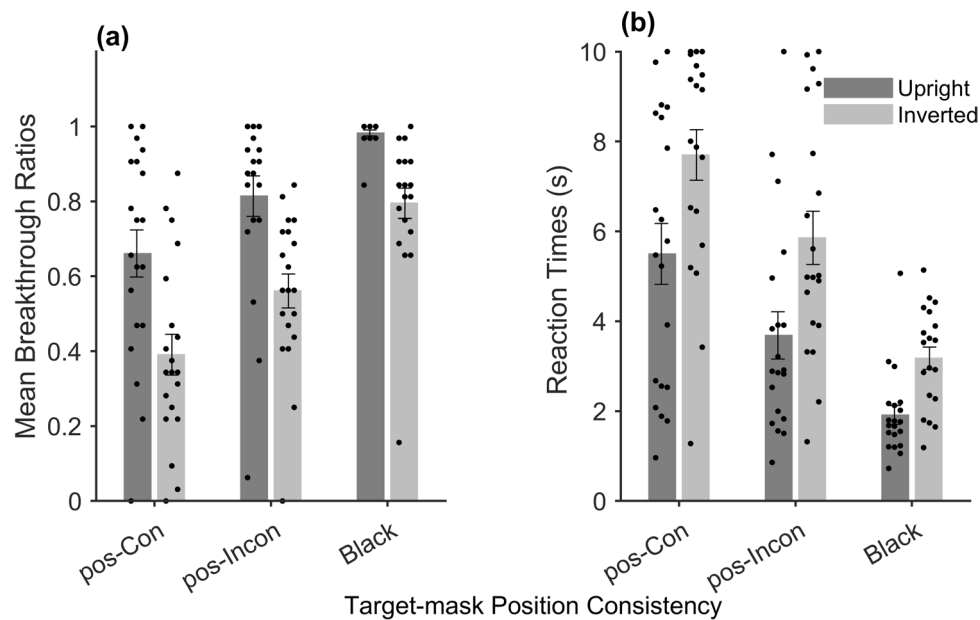


Fig. 5 Results for Study 2b. *Note.* Error bars represent ± 1 SEM. pos-Con, position-consistent condition; pos-Incon, position-inconsistent condition. The dots show the individual data. The results of (a)

breakthrough ratios and (b) median RTs across target-mask position consistency in Study 2b.

Interim discussion

To optimize the masking efficacy for BM stimuli, we developed the Chameleon-2 paradigm. Studies 2a and 2b systematically investigated the masking effects of this paradigm by examining target-mask color consistency and position consistency.

Our findings revealed that color influenced the masking efficacy of Chameleon-2, but this effect was driven by the global color pattern of the target stimuli rather than the specific color of individual light points. Specifically, a colored pattern enhanced masking intensity compared to an achromatic pattern. Critically, Study 2a demonstrated that Chameleon-2 generated significantly stronger masking effects on BM stimuli. By using a classic CFS paradigm to present low contrast BM stimuli for 2 s per trial (ramped up from zero to 10% contrast for 900 ms and maintained for 1100 ms), previous work achieved a breakthrough ratio of ~ 67% (estimated according to their d' results, Sun et al., 2022). As a more direct comparison, the breakthrough ratios re-calculated within the first 2-s window in trials of Study 2a were as low as 15.96%. This masking efficacy is far better than both the classic CFS paradigm and Chameleon-1. Bear in mind, our Chameleon-2 paradigm allowed abrupt presentation of full-contrast BM stimuli for 10 s. Considering the high contrast energy of the target throughout the entire trial length, this way of presenting targets is supposed to be more challenging than the contrast-ramping manner in the classic CFS paradigm.

Study 2b also achieved low breakthrough ratios (14.92%) within the initial 2-s window of trials, replicating the finding in Study 2a. Moreover, Study 2b demonstrated that maximal masking efficacy required precise spatial alignment between the BM light points and their corresponding masking elements. Complete position consistency enabled full perceptual fusion between the BM stimuli and masking patterns, yielding significantly stronger masking. Conversely, position inconsistency led to interocular conflict by superimposing light points onto the gray background in the opposite eye. Such interocular mismatch reduced masking effectiveness. These results identify position consistency as a critical determinant of optimal masking performance in the Chameleon-2 paradigm. Importantly, both Studies 2a and 2b demonstrated significant inversion effects (e.g., in Study 2a, inverted: breakthrough ratios = ~ 50%, median RTs = 7 s; upright: breakthrough ratios = ~ 83%, median RTs = 4 s), verifying that the Chameleon BM stimuli maintained the essential BM information (Troje & Westhoff, 2006). Notably, the inversion effect was markedly stronger in the color-consistent/position-consistent condition than in the black condition, likely attributable to extended masking duration facilitated by target-mask feature consistency—a finding congruent with Gayet and Stein's (2017) observation that prolonged masking enhances the inversion effects.

Moreover, one may argue that breakthroughs are simply due to imperfect binocular fusion rather than accumulation of subliminal sensory evidence. However, the eye movement data of Study 2c showed no significant differences in

the fixation disparity between the breakthrough and non-response trials, nor were there any discernible fluctuations in the fixation disparity patterns across the trial types, providing compelling evidence against the argument of fusion instability (see Section S5 of the supplementary information). Rather, we propose that participants could successfully extract and process BM information even under complete fusion, with this unconscious processing ultimately leading to perceptual breakthrough. Building upon our validated Chameleon-2 paradigm for BM masking, we then utilized this optimized paradigm to explore unconscious BM processing in Study 3.

Study 3: Application of the Chameleon-2 Paradigm

To our best knowledge, the Chameleon-2 paradigm, for the first time, allows efficient masking (< 16% breakthroughs within the first 2 s) of high-contrast BM stimuli. The relatively long masking duration and presentation of high-contrast target stimuli throughout a trial makes Chameleon-2 a promising candidate paradigm for neuroimaging research to explore the neural correlates of unconscious BM processing. Nevertheless, to avoid difficulties in interpreting potential negative results from experiments measuring unconscious BM processing, we decided that in Study 3a, we would measure brain activity in response to the Chameleon BM targets but without presenting the masks (i.e., under a conscious level). Afterwards, Study 3b would measure any potential brain activity for unconscious BM processing with both the masks and BM stimuli presented.

Study 3a: Conscious processing of Chameleon BM

When creating the Chameleon BM stimuli, the light points of the BM targets were repositioned to align with the mask patterns. This would inevitably add a certain degree of noise to the targets. Study 3a first assessed the BM-processing related rSTS activation during conscious perception of the Chameleon BM targets (without the masking stimuli) to confirm that BM signal is detectable even with the added noise.

Method

Participants We recruited thirty participants (11 males and 19 females, $M_{\text{age}} = 22.40$ years, age range 19–26 years) in Study 3a. The number of participants in Study 3 was predetermined based on the sample sizes of recent fNIRS studies on BM (Lisboa et al., 2020a, 2020b).

Stimuli Stimuli were displayed on a gamma-corrected 27-inch HP 27Y monitor (1920 × 1080 pixel resolution,

refresh rate: 60 Hz, average brightness: 41.82 cd/m²). White stimuli (RGB: [255 255 255]) were presented on a black background (RGB: [0 0 0]). No masking stimulus was presented in this experiment, thus the participants directly viewed the BM stimuli displayed at the central fixation point. Four BM stimulus types (left/right directions) were used: (1) intact BM (original PLW from Study 2); (2) scrambled BM (randomized point positions with preserved trajectories via BioMotion Toolbox); (3) Chameleon BM (identical to Study 2); (4) Chameleon scrambled BM (scrambled reconstruction using masking element positions).

fNIRS data acquisition Hemodynamic data were acquired using a LABNIRS system (Shimadzu Inc., Japan), recorded at near-infrared wavelengths 780/805/830 nm and 55.56-Hz sampling (18 ms sampling interval). Prior to recording, we localized the ROIs (STS) using the transcranial imaging and neural regulation dual navigation system (Xiao et al., 2018). This procedure involved first obtaining scalp surface topography for each participant, followed by computation of STS coordinates through co-registration of the international 10–20 system with the anatomical automatic labeling (AAL) atlas. The optode configuration was then carefully adjusted to these coordinates to ensure optimal coverage of the ROIs. The final optode configuration was centered on FC5 and FC6 according to the international 10–20 system, with bilateral 3 × 3 grid configurations (five sources and four detectors per hemisphere) maintaining an inter-optode distance of 30 mm. This arrangement generated 12 channels per hemisphere (24 channels total), providing coverage of bilateral temporal-parietal regions with extension into adjacent frontal areas (see Fig. 6).

Following data collection, we performed post-experiment optodes localization using a Fastrak 3D tracking and digitizing system (Polhemus Inc., VT). For each participant, we recorded the spatial coordinates of all optodes along with four anatomical landmarks: the nasion (Nz), vertex (Cz), and bilateral preauricular points (AL and AR). These localization data were then co-registered with standard brain templates from the Montreal Neurological Institute (MNI) to: (1) compute the precise spatial coordinates of each channel, and (2) evaluate their corresponding cortical subdivisions.

Procedure Participants viewed stimuli from 80 cm with head position stabilized using a forehead rest. The experiment employed a block design consisting of 32 blocks (eight blocks per condition), each containing ten trials (five with leftward and five with rightward movement directions) presented in a pseudo-random order. Each trial began with a 500-ms presentation of a white fixation cross, followed by a 1.6-s BM stimulus displaying one complete gait cycle. During the stimulus presentation, participants monitored

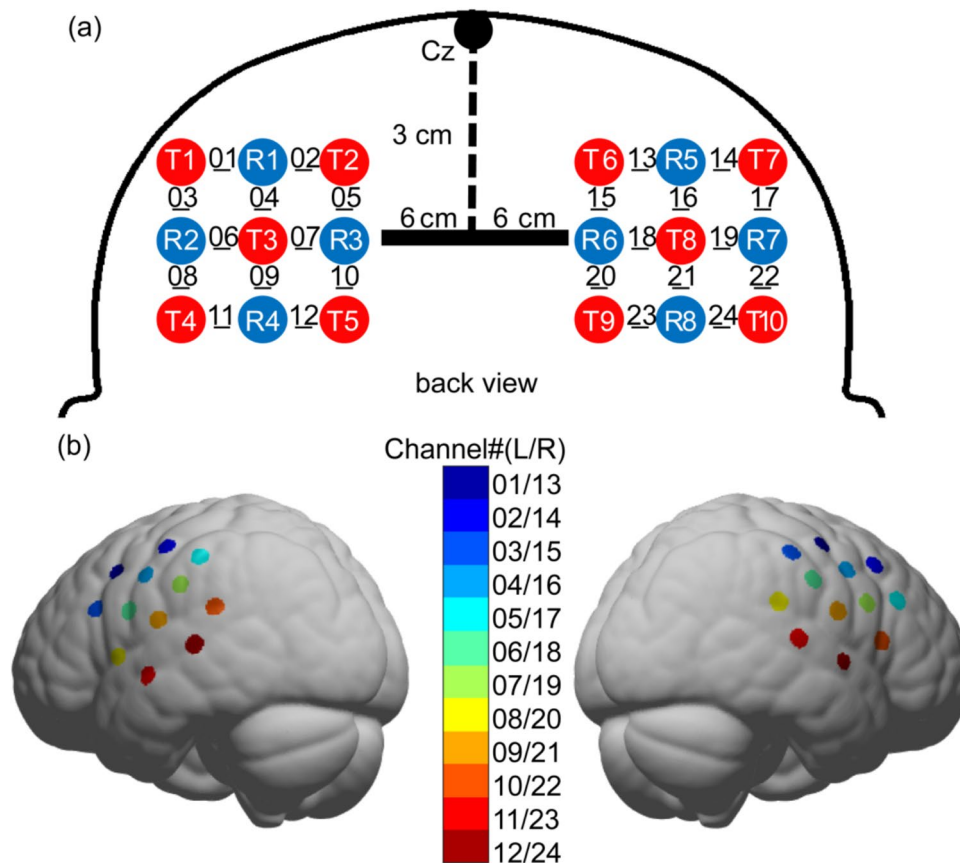


Fig. 6 Optode configuration for Study 3. *Note.* (a) The optode arrangement consisted of emitter–detector pairs, with emitters (T) indicated by red symbols and detectors (R) shown in blue. Adjacent emitter–detector pairs were spaced 30 mm apart to form measurement channels (*underlines*). Each cerebral hemisphere contained 12 chan-

nels, yielding a total of 24 channels. *Dotted lines* indicate geodesic distances along the scalp relative to Cz (*vertex*). All schematic elements are representational and not drawn to scale. (b) Corresponding spatial distribution of the 24 channels projected onto a standard brain template.

the fixation point for 200-ms color changes (from red to green, randomly between 0.5 and 1.1 s post-stimulus onset; see Figure S8, in Section S6 of the supplementary information), responding via the spacebar. Inter-block rests lasted no less than 18 s. The fNIRS data were acquired continuously during the ~ 20-min task, with the total session duration (including preparatory setup, practice, and post-experiment optode localization) reaching approximately 80 min.

Analysis The acquisition system provided raw measurements, including absorbance at each near-infrared wavelength and hemodynamic parameters (oxygenated hemoglobin (HbO), deoxygenated hemoglobin (HbR), and total hemoglobin). The fNIRS and localization data were processed and analyzed using NIRS-KIT v2.0 (Hou et al., 2021, integrated with MATLAB, The MathWorks, Natick, MA, USA). The analysis consisted of four major steps: (1) data organization, (2) preprocessing, (3) spatial localization analysis, and (4) analysis of hemodynamic signal changes.

The initial data organization stage involved extracting baseline epochs (2-s pre-stimulus windows) and experimental epochs (20-s post-stimulus periods) for each experimental condition. Preprocessing followed the methodology described by He and Bao (2024). For details, see Section S6 of the supplementary information.

In the spatial localization analysis, we first processed the post-experiment Fastrak coordinate data by computing the mean positions of four reference points and 24 channels across participants. These averaged positions were transformed to MNI coordinates using NIRS-KIT. Then we performed probabilistic anatomical mapping against the AAL atlas, assigning each channel to the brain region showing the highest probability of overlap.

Hemodynamic analysis involved computing condition-wise mean HbO/HbR concentrations across channels at each timepoint. These time-series data were then compared to their corresponding baselines using paired-sample *t* tests to identify significant hemodynamic fluctuations. We restricted

our analysis to significant increases in HbO concentrations and decreases in HbR concentrations. Temporal patterns of significant activation ($p < 0.05$, uncorrected) were used to define time windows for subsequent analysis. Within these time windows, we calculated the mean hemodynamic amplitude for each condition, focusing on channels within predefined ROIs. To address multiple comparisons, false discovery rate (FDR) correction was applied separately for each hemisphere, with the threshold adjusted according to the number of ROI channels. Statistical comparisons between conditions were only performed when at least two conditions exhibited significant hemodynamic changes after correction. Our analysis included an exploratory examination of non-ROI channels (see Section S6 of the supplementary information for details).

Results

After preprocessing, 1.45% of data blocks were excluded based on the quality control criteria. Temporal analysis of

mean hemodynamic responses across all channels revealed condition-specific patterns. Compared to baseline ($p < 0.05$, uncorrected), significant HbO concentration increase clustered in two distinct phases: an early synchronized response (2–6 s) across all conditions, and a later sustained activation (12–18 s) exclusive to intact and scrambled Chameleon BM conditions (see Fig. 7). No significant HbR concentration decrease was detected. Based on established literature demonstrating HbO's superior sensitivity in detecting neural activation (Lloyd-Fox et al., 2010; Strangman et al., 2002), subsequent analysis focused on these two HbO time windows (2–6 s and 12–18 s).

Guided by our hypothesis that the STS underlies BM processing, we focused on its activation. Although fNIRS cannot directly resolve the STS due to limited spatial resolution (Pinti et al., 2020), hemodynamic responses in the superior temporal gyrus and middle temporal gyrus likely reflect concurrent STS activation through shared vasculature. Therefore, optode localization mapped channels 8, 10–12 to the left STS (lSTS), and channels 20, 23–24 to the rSTS.

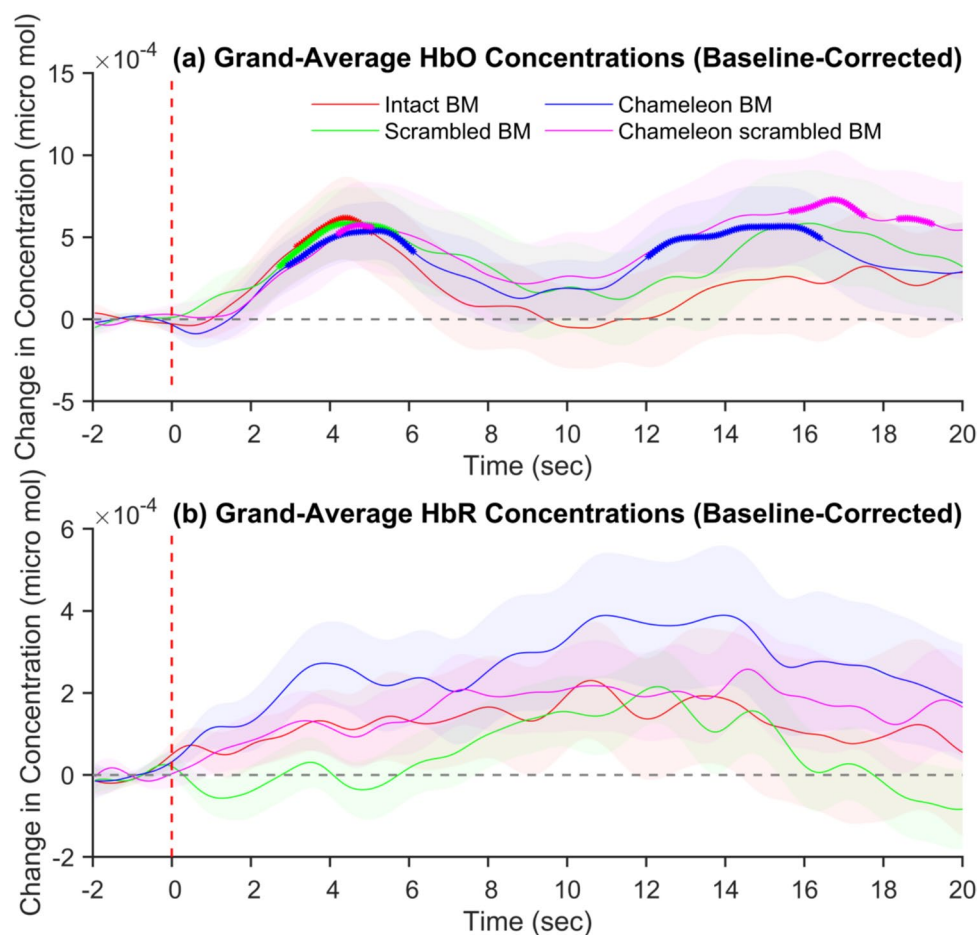


Fig. 7 Grand average of baseline-corrected HbO and HbR concentrations in Study 3a. *Note.* The *gray dashed line* indicates baseline level, while the *red dashed line* marks stimulus onset. Time points with

statistically significant deviations from baseline (HbO concentrations increase/HbR concentrations decrease; $p < 0.05$, uncorrected) are marked with *asterisks*.

Paired sample t tests of HbO concentrations change during the 2–6-s time window revealed similar activation patterns across conditions (see Fig. 8a). Intact BM stimuli activated both ISTS and rSTS, though only the rSTS activation survived the FDR correction. Scrambled BM stimuli selectively activated the rSTS. Chameleon BM stimuli mirrored intact BM's bilateral activation pattern but only the rSTS survived the FDR correction. Chameleon scrambled BM stimuli showed uncorrected bilateral activation. Repeated measures ANOVA revealed no significant differences in activation between the conditions ($F_{(3, 87)} = 0.600$, $p = 0.616$, $\eta_p^2 = 0.020$).

Late-phase HbO analysis (12–18 s) showed condition-specific activation patterns (see Fig. 8b). Scrambled BM selectively activated the rSTS, while Chameleon BM elicited significant ISTS activation. Its scrambled version showed uncorrected activation in bilateral STS regions. Intact BM showed no late-phase activation ($t_{(29)} \leq 1.594$, $p_{\text{uncorr}} \geq 0.122$), suggesting earlier completion of core processing for this condition. Complete results are summarized in Table 6.

Interim discussion

Individual light points in the Chameleon BM stimuli are spatially shifted, yet they oscillate around the underlying

skeletal structure, thereby preserving both a certain degree of local motion and global configurational information. By using the fNIRS technique, Study 3a revealed that the consciously presented Chameleon BM stimuli (masks not displayed) activated the rSTS, a key region for BM processing (e.g., Allison et al., 2000; Lisboa et al., 2020a, 2020b; Troje, 2013; Wang et al., 2023) rather than non-BM (e.g., mechanical movements, Pelphrey et al., 2003; Pelphrey & Morris, 2006). This indicates that these stimuli indeed preserve sufficient BM features to engage specialized visual processing mechanisms. Crucially, scrambling the Chameleon BM—which disrupts its global structure—substantially reduced the rSTS activation, though a weak residual response persisted that did not reach FDR-corrected significance.

In addition, scrambled BM stimuli—which disrupt spatial configuration but preserve local motion trajectories—activated the rSTS in our study. This result contributes to an ongoing debate in the literature. Some studies report absent or weak rSTS responses to scrambled BM (Peuskens et al., 2005; Lisboa et al., 2020b), while others report significant activation, albeit often reduced compared to intact BM (Saygin et al., 2004; Jastorff & Orban, 2009). Our findings support the view that local motion within scrambled BM stimuli can still engage the rSTS, consistent with the

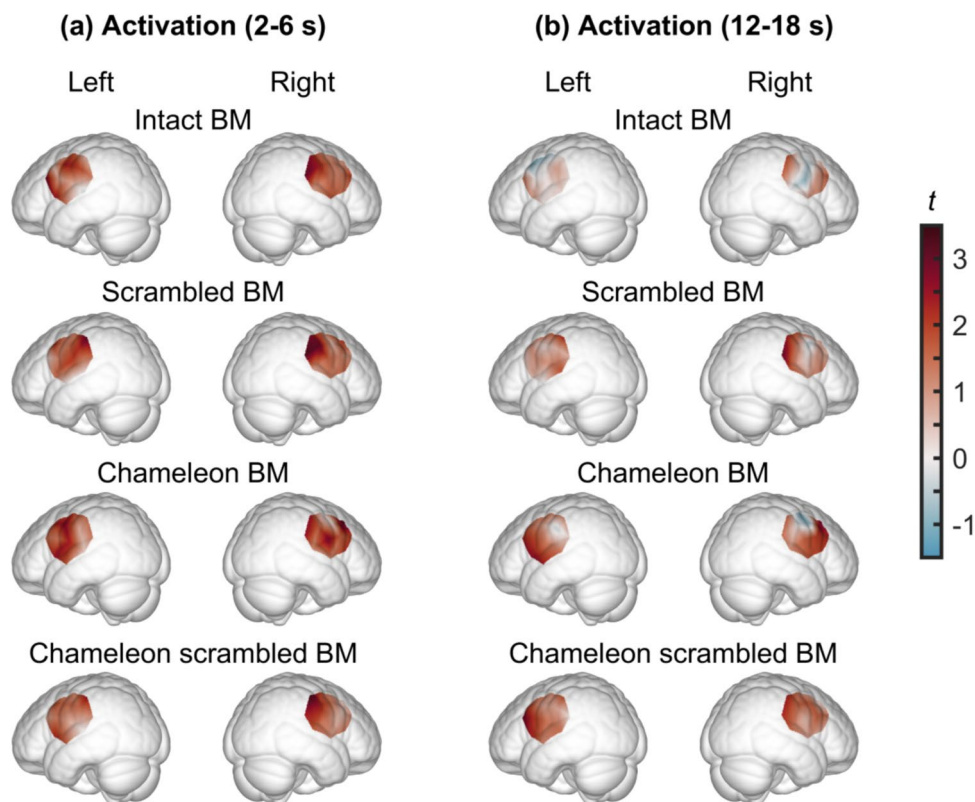


Fig. 8 Distribution of HbO activation at two time windows in Study 3a

Table 6 Results for Study 3a

Time window	Condition	Channel	MNI	Regions	$t_{(29)}$	p_{uncorr}	p_{FDR}	d
2–6 s	Intact BM	8	[− 62, 4.333, 2.333]	ISTS (0.395)	2.572	0.016	n.s.	0.470
		20	[70, − 39.667, 24.333]	rSTS (0.527)	3.224	0.003	< 0.05	0.589
	Scrambled BM	20	[70, − 39.667, 24.333]	rSTS (0.527)	3.338	0.002	< 0.05	0.609
		Chameleon BM	8	[− 62, 4.333, 2.333]	ISTS (0.395)	2.497	0.019	n.s.
	Chameleon scrambled BM	20	[70, − 39.667, 24.333]	rSTS (0.527)	2.596	0.015	< 0.05	0.474
		8	[− 62, 4.333, 2.333]	ISTS (0.395)	2.338	0.027	n.s.	0.427
12–18 s	Scrambled BM	20	[70, − 39.667, 24.333]	rSTS (0.527)	3.215	0.003	< 0.05	0.587
		Chameleon BM	8	[− 62, 4.333, 2.333]	ISTS (0.395)	2.635	0.013	< 0.05
	Chameleon scrambled BM	11	[− 69, − 11.667, − 8.333]	ISTS (0.981)	2.415	0.022	< 0.05	0.441
		8	[− 62, 4.333, 2.333]	ISTS (0.395)	2.381	0.024	n.s.	0.435
	Chameleon scrambled BM	20	[70, − 39.667, 24.333]	rSTS (0.527)	2.320	0.028	n.s.	0.424

Only increases in HbO concentrations were found and presented. The anatomical regions were defined according to the AAL atlas. Probabilities for each region are shown in parentheses. ISTS = left superior temporal sulcus; rSTS = right superior temporal sulcus; BM = biological motion; p_{uncorr} = uncorrected p values; p_{FDR} = false discovery rate-corrected p values; n.s. = not significant.

model proposing integrative motion processing in this region (Giese & Poggio, 2003).

In fact, the preservation of BM information across these four stimulus types can be characterized along two dimensions: local motion and global configuration. The intact BM preserves both; the scrambled BM preserves only local motion but lacks global configuration; the Chameleon BM incorporates spatial perturbations in both local and global features; the Chameleon scrambled BM combines these perturbations with a complete loss of global configuration. Therefore, the rSTS activation patterns in the four experimental conditions suggest that this region encodes BM information in a graded manner, relying on both local motion and global configurational cues.

Interestingly, the Chameleon BM stimuli also activated the ISTS, another well-established region in BM processing (Herrington et al., 2011; Peelen & Downing, 2007; Puce & Perrett, 2003). This bilateral STS activation pattern contrasts with the right-lateralized STS response to the intact or scrambled BM stimuli, which may result from the novel perceptual demands of the Chameleon BM to integrate the global structure with the local motion perturbations. Actually, the pattern aligns with proposals that BM processing initially involves the bilateral STS, with the right-hemisphere dominance strengthening through perceptual experiences (Grossmann, 2015; Lisboa et al., 2020a).

Study 3b: Unconscious processing of Chameleon BM

Given the clear neural evidence from Study 3a that the Chameleon BM stimuli preserve relevant BM properties under the conscious viewing conditions, Study 3b was designed to

investigate the neural correlates of its unconscious processing using masking.

Method

Participants We recruited 30 participants (12 males and 18 females, $M_{\text{age}} = 21.13$ years, age range 18–24 years) in Study 3b.

Stimuli The experimental setups, including equipment and optode configuration, were identical to Study 3a. The stimuli for Study 3b replicated that of Study 2a, comprising: masking stimuli and Chameleon BM stimuli.

Procedure The experiment involved two sessions (≥ 48 h apart). Session 1 included eye-dominance testing (replicating Study 1) and fNIRS acquisition using a protocol similar to Study 3a (see Figure S8, in Section S6 of the supplementary information). Participants completed 30 blocks (15/condition) in pseudo-random order: (1) Mask-only condition—only the dominant eye received masking stimuli; (2) BM-present condition—the dominant eye viewed masks while the non-dominant eye saw the Chameleon BM stimuli. Each trial began with a variable-duration mask (100/200/300/400 ms) in the dominant eye. Subsequently, while the dominant eye continued to display the masking stimulus for an additional 1.6 s, the non-dominant eye was exposed to either a Chameleon BM stimulus or a fixation point. Although the short 1.6-s exposure duration made perceptual breakthroughs not very likely (per Study 2 findings), participants were nevertheless instructed to report the perceived direction of PLW whenever detected. To accommodate this, we implemented a dual-response paradigm

consisting of: (1) a fixation monitoring task (presented in 50% of trials per block) requiring the left-hand spacebar responses (same as Study 3a), and (2) a direction discrimination task requiring the right-hand arrow key responses upon conscious detection of BM stimuli. Importantly, the responses to the fixation task did not terminate the stimuli presentation, while the directional responses served as our primary behavioral measure of subjective awareness. Furthermore, to verify unconscious processing states, two counter-balanced two-alternative forced-choice (2AFC) awareness tests were administered in Session 2 (see Section S7 of the supplementary information for details). This approach provides an objective measure of participants' conscious awareness states during the experiment.

Analysis Participants were classified into distinct groups using two complementary methods to dissociate unconscious and conscious processing of BM stimuli: (1) Subjective measures of conscious awareness: Participants were categorized based on behavioral responses collected during the fNIRS acquisition. The non-response group was defined as the participants contributing at least five blocks without any behavioral response (reflecting potential unconscious processing), whereas the breakthrough group included those who achieved correct PLW direction discrimination in at least three out of ten trials in one or more blocks. Subsequent analyses were conducted on non-response blocks (exclusively from the non-response group) and breakthrough blocks (exclusively from the breakthrough group). (2) Objective measures of conscious awareness: Participant classification was performed based on the performance in the second awareness test (a BM direction discrimination task; see Section S7 of the supplementary information for details), applying the established criterion that detection without discrimination reflects unconscious processing (Stein & Peelen, 2021). Consistent with prior operational definitions (Goldstein et al., 2020), participants performing below the discrimination threshold (< 60% accuracy) on BM trials were classified as the unconscious group; while the remaining participants were assigned to the conscious group (refer to Figure S10b, in Section S7 of the supplementary information).

While subjective methods are considered not bias-free, objective methods (e.g., 2AFC) are criticized for: (1) risking overestimating conscious knowledge, since above-chance performance may be due to unconscious knowledge rather than conscious (Dong et al., 2022; Timmermans & Cleeremans, 2015), and (2) potential incomparability of attentional states between the 2AFC tasks and the b-CFS paradigms (Dong et al., 2022; Vermeiren & Cleeremans, 2012). To address these complementary limitations, the present study employed both subjective and objective measures to classify

participants, enabling the examination of the neural correlates of unconscious and conscious BM processing.

Hemodynamic analysis followed Study 3a's analytical framework, applying its predefined time windows to examine condition-specific HbO/HbR dynamics across groups. Given the introduction of masking stimuli in Study 3b, we applied FDR correction with the correction threshold determined by the number of channels within each hemispheric region.

Results

We found consistently low behavioral breakthrough ratios across participants (0.10 ± 0.03) during the fNIRS recordings. This result further supported the effectiveness of the Chameleon-2 paradigm in masking BM stimuli.

After preprocessing, 1.42% of data blocks were excluded based on the same quality control criteria as in Study 3a. Based on the subjective measures of conscious awareness, 22 participants met the criteria for the non-response group (contributing at least five valid non-response blocks), while nine participants qualified for the breakthrough group (demonstrating correct responses in at least three out of ten trials per block in one or more blocks). One participant qualifying for both groups was excluded from the non-response cohort to preserve unconscious processing measures (final $N = 21$). However, based on objective measures of conscious awareness, ten participants were classified into the unconscious group (showing below-threshold discrimination accuracy, < 60%, for BM trials), while the remaining twenty participants were assigned to the conscious group.

As noted by Timmermans and Cleeremans (2015), above-chance performance in objective awareness tests can stem from both conscious and unconscious processes. Notably, nearly half of the participants classified as "conscious" under the objective measure exhibited low breakthrough ratios (see Figure S10c, in Section S7 of the supplementary information). These participants often failed to report subjective awareness despite meeting the objective criteria, suggesting that the objective classification may lack the sensitivity needed to reliably differentiate conscious perception from unconscious processing in the Chameleon paradigm which required different attentional states from the 2AFC task (for a similar view, see Dong et al., 2022; Vermeiren & Cleeremans, 2012). Given these findings, we focused specifically on the grouping derived from the subjective measures, as this participant classification appeared to more accurately reflect the distinct states of genuine conscious perception. Results pertaining to the objectively defined unconscious and conscious groups are provided in Section S7 of the supplementary information.

Hemodynamic analyses employed Study 3a's time windows (2–6 s and 12–18 s). Group-wise time-course plots

revealed significant HbO increases relative to baseline ($p < 0.05$, uncorrected) peaking within these windows across all participants (see Fig. 9 and Figure S11, in Section S7 of the supplementary information), with no corresponding HbR changes (see Figure S13, in Section S7 of the supplementary information). Consequently, subsequent analyses focused exclusively on the HbO data. We report only the activation results within the predefined ROIs. Comprehensive results and extended discussions of the non-ROIs activations are provided in Sections S7 and S8 of the supplementary information.

The non-response group displayed no significant ROI activation during either the 2–6 s or 12–18 s time windows in either the mask-only or BM-present conditions ($t_{(20)} \leq 0.892$, $p_{\text{uncorr}} \geq 0.383$, $d \leq 0.195$, see Fig. 10a). In contrast, the breakthrough group maintained selective activation of the rSTS that was exclusively observed in the BM-present condition during both the 2–6 s and 12–18 s time windows (see Fig. 10b and Table 7).

Interim discussion

Study 3b further explored the neural correlates of unconscious BM processing with the Chameleon-2 paradigm. For

the BM-present condition, robust activation of the rSTS was observed specifically in the breakthrough group, while no such activation was detected in the non-response group. Neither group exhibited significant ROI activation in the mask-only condition.

How to explain the selective STS activation under the BM-present condition in the breakthrough group? We propose two possible explanations here and a third, more speculative explanation in Section S8 of the supplemental information. First, STS activation may require conscious awareness of BM stimuli. This is based on the fact that participants in the breakthrough group consciously detected the BM stimuli and exhibited the STS activation, whereas those in the non-response group neither detected the BM consciously nor showed such activation. Notably, the interpretation aligns with Kim and colleagues' (2011) finding that even non-BM stimuli can evoke STS activity when these stimuli were mistakenly perceived as BM. Further evidence comes from Kim et al. (2013)'s fMRI work that examined unconscious BM processing. They found STS activation only when participants were consciously aware of the BM stimuli, but not in the absence of awareness. These results collectively suggest that STS activation depends on conscious perception of BM regardless of the presence of BM stimuli. Alternatively, STS neurons could respond to

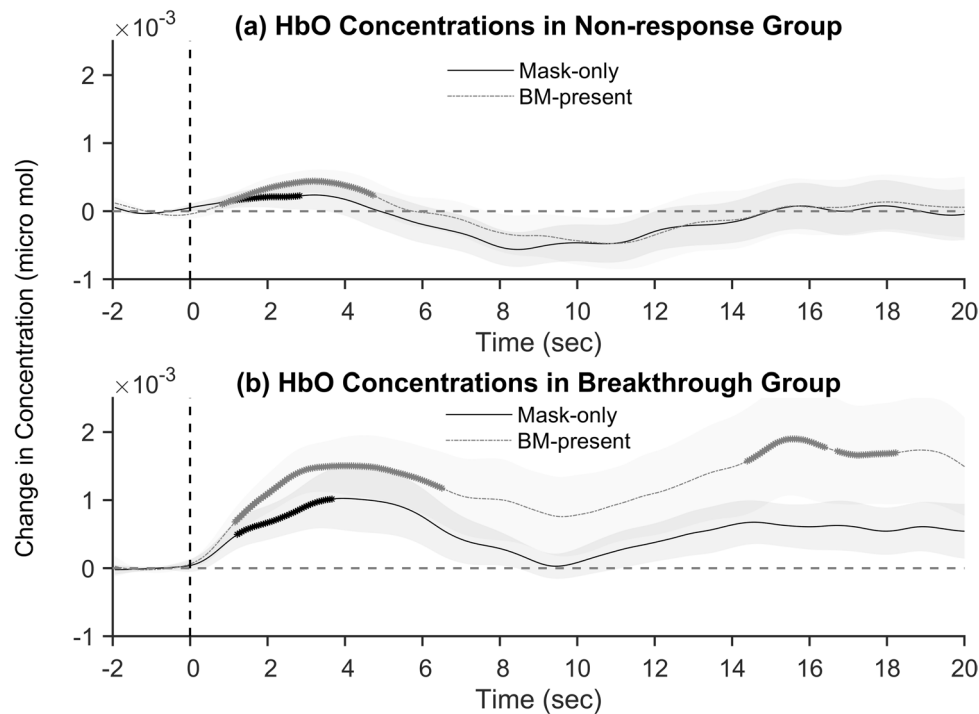


Fig. 9 Grand average of baseline-corrected HbO concentrations for the subjective grouping in Study 3b. *Note.* The horizontal gray dashed lines indicate the baseline level, while the vertical black dashed line marks the stimulus onset. Time points exhibiting statistically significant increases in HbO concentrations ($p < 0.05$, uncorrected) are marked with asterisks. The mask-only condition is

denoted by the *black line*. **(a)** Results from the non-response group. The gray line indicates the data derived exclusively from the non-responding blocks in the BM-present condition. **(b)** Results from the breakthrough group. The gray line indicates the data derived exclusively from the breakthrough blocks in the BM-present condition.

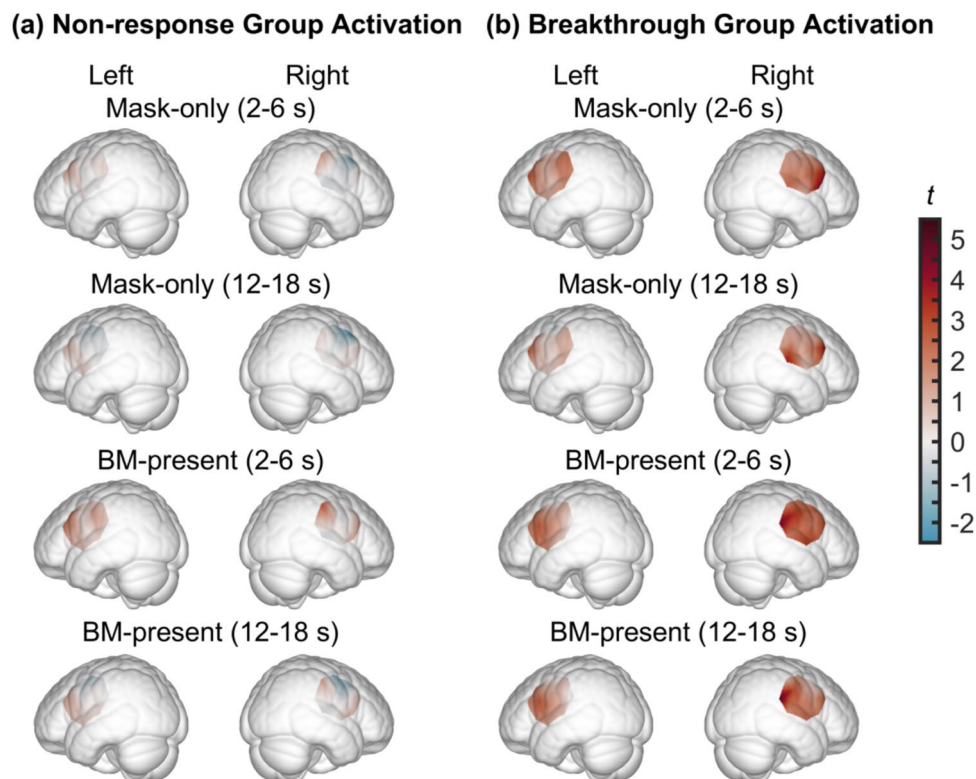


Fig. 10 Distribution of HbO activation at two time windows for the subjective grouping in Study 3b

Table 7 Results for the breakthrough group in Study 3b

Time window	Channel	MNI	Regions (probabilities)	$t_{(8)}$	p_{uncorr}	p_{FDR}	d
2–6 s	20	[69, -45.333, 21.333]	rSTS (0.614)	4.651	0.002	< 0.05	1.550
	24	[71, -11.667, -3.667]	rSTS (0.676)	3.323	0.011	< 0.05	1.108
12–18 s	20	[69, -45.333, 21.333]	rSTS (0.614)	5.127	< 0.001	< 0.05	1.709

Only significant increases in HbO concentrations in the BM-present condition for the breakthrough group were found and presented here. The anatomical regions were defined according to the AAL atlas. rSTS = right superior temporal sulcus; p_{uncorr} = uncorrected p -values; p_{FDR} = false discovery rate-corrected p values.

unconscious BM stimuli, yet the attenuated neural representation of these signals may fall below the detection threshold of fNIRS. This explanation is consistent with previous fMRI findings showing significantly reduced blood-oxygen-level-dependent signals for unconscious processing of tool images relative to conscious perception (Hesselmann & Malach, 2011).

General discussion

Across three studies, we systematically developed and validated the novel Chameleon-2 paradigm for robust and sustained masking of BM stimuli. Study 1 revealed that the

Chameleon-1 paradigm effectively masked slower, larger-sized multi-point translational targets at various contrasts, but not for complex BM patterns. Building hereon, Study 2 introduced Chameleon-2, which successfully masked BM stimuli by maintaining critical color and spatial consistencies between the targets and masks. Study 3 confirmed that the Chameleon BM stimuli elicited the rSTS activation resembling intact BM, demonstrating preserved BM information. Together, these findings establish the Chameleon-2 paradigm as a reliable method for investigating unconscious motion processing.

Although both Chameleon paradigms enable long-duration motion masking, they differ in applicability. Chameleon-1 is effective for slower translational motion but proves

ineffective for faster BM stimuli that incorporate complex kinematic and social information, as shown by the near-ceiling breakthrough ratios ($\sim 100\%$) and short median RTs (~ 2 s). In contrast, Chameleon-2 significantly improves BM masking. Strikingly, both Studies 1 and 2 used 10-s exposures to assess temporal robustness of masking—a duration far exceeding typical BM presentation times in literature (e.g., one step cycle, 500–2000 ms). Study 3b also confirmed that Chameleon-2 maintains high masking efficacy at 1.6 s (one-step cycle), with a notably low breakthrough ratio ($M = 9.89\%$, $SE = 3.24\%$). Although Chameleon-1's masking efficacy decreases for faster motion, it may still be applicable under specific parameters (e.g., shorter durations; slow-moving or static targets). Nonetheless, its limitations underscore Chameleon-2's advantage for masking high-speed stimuli.

Beyond differences in motion masking efficacy, the two paradigms also diverge in their reliance on color consistency. While critical for masking in the Chameleon-1 paradigm (Zhao & Bao, 2022), color consistency provided no significant benefit in Chameleon-2. This discrepancy may be due to different experimental parameters. Chameleon-1 employed slowly moving stimuli ($0.2^\circ/\text{s}$) with a 10-Hz color refresh rate, whereas Chameleon-2 involved faster BM stimuli ($> 0.2^\circ/\text{s}$) and a 60-Hz refresh rate. Under these dynamic conditions, color processing is constrained by known temporal limits—color discrimination declines at higher velocities in the CFS paradigms (Hong & Blake, 2009) and is impaired by high-frequency flicker (Wu et al., 2019). Furthermore, color processing in area V4 (Liu et al., 2020) requires integration time exceeding 16.67 ms (60-Hz refresh rate). Consequently, under the Chameleon-2's faster regime, participants lacked sufficient temporal resolution to utilize the color cues, negating the contribution of color consistency to masking efficacy.

One may question whether the spatial realignment of BM stimuli in Chameleon-2 reduces biologically relevant motion information. Although this method inevitably perturbs some BM features, this trade-off is necessary to achieve effective masking. Importantly, two key findings confirm that the generated stimuli retain functionally meaningful information: the robust inversion effect (Study 2) and the significant rSTS activation during conscious perception (Studies 3a and 3b). These results demonstrate that although some information loss occurs, the residual BM signal remains sufficient to support stable perceptual processing. Thus, the paradigm represents a carefully optimized balance between maintaining essential BM characteristics and ensuring reliable masking efficacy.

Given the limitation that the paradigm reduces certain aspects of BM information, future work could adaptively modulate the motion signal strength based on the required masking duration. For instance, the spatial density of mask elements can be increased to raise the signal-to-noise ratio

for shorter trials. A second limitation is the use of separate participant groups in Studies 3a and 3b, which precludes a within-subject comparison between conscious and unconscious processing of BM. Our reason is that we first verified that the novel Chameleon BM stimuli exhibited BM properties when consciously perceived before examining unconscious processing. However, to avoid any potential carryover or learning effects between experimental sessions (Gayet et al., 2013; Mastropasqua et al., 2015; Paffen et al., 2018), we had to run Studies 3a and 3b in separate groups. Future studies may employ within-subject designs to enable direct comparisons between conscious and unconscious conditions.

The primary contribution of this study is the introduction of the Chameleon paradigms, which can stably mask motion stimuli over extended durations. The distinctive design offers broad applicability across research contexts. Unlike classical CFS with gradual contrast buildup, the Chameleon paradigms present targets at full contrast from the onset, enabling precise control of duration and intensity while maintaining effective masking. This ensures robust input strength for the target, making it particularly suitable for unconscious perception research. For example, it allows strong masking of the prime in unconscious priming paradigms, meanwhile sufficient stimulus strength ensures effective priming. It also guarantees a higher duty cycle for the adapter during top-up motion adaptation studies, potentially boosting adaptation effects. In neuroimaging studies (e.g., our Study 3b), the use of high-contrast stimuli throughout each trial ensures that a lack of brain activation in the unconscious condition cannot be readily attributed to suboptimal stimulus strength, thereby strengthening the interpretation of null results. Moreover, because masks are generated from purely random motion patterns without meaningful structure, they avoid carrying target-like features. This clear separation ensures that neural responses can be confidently attributed to target processing, extending the paradigm's utility for investigating unconscious processing of diverse types of complex motion, such as optic flow and self-motion, social actions and interactions, object motion and function, anomalous or physics-violating motion, etc.

Conclusion

This study introduces the Chameleon paradigms—a methodological advance enabling robust, sustained masking of complex motion stimuli. The Chameleon-1 paradigm effectively masks slow, large-element translational motion, while the Chameleon-2 extension overcomes the challenge of masking BM, as empirically established in Studies 2 and 3. The fNIRS recordings confirmed that the Chameleon BM stimuli recruited core BM-processing regions exclusively during conscious perception, highlighting the paradigm's capacity

to dissociate neural correlates of awareness. By bridging a critical gap in dynamic motion masking, this work provides a powerful tool for probing the temporal dynamics and neural foundations of unconscious motion processing.

Supplementary Information The online version contains supplementary material available at <https://doi.org/10.3758/s13428-025-02924-8>.

Acknowledgements We greatly appreciate the excellent work of the technical support staff at the Institutional Center for Shared Technologies and Facilities of the Institute of Psychology, Chinese Academy of Sciences.

Authors' contributions M.B. and Y.J. conceptualized the research; J.Z., M.B., and Y.J. designed the experiments; J.Z. performed the experiments; J.Z. and X.H. analyzed the data; and J.Z., M.B., and Y.J. wrote the article.

Funding This research was supported by the Brain Science and Brain-like Intelligence Technology - National Science and Technology Major Project (2021ZD0203800) and the National Natural Science Foundation of China (32471106, 32430043, and 32300878).

Availability of data and code The datasets and code generated during the current study are available in the Science Data Bank repository. <https://www.scidb.cn/s/nEJnQn>

Declarations

Ethics approval This study was performed in line with the principles of the Declaration of Helsinki. Approval was granted by the Institutional Review Board of the Institute of Psychology, Chinese Academy of Sciences.

Consent to participate and publish All participants provided written informed consent for both study participation and the publication of anonymized data.

Open practices statement None of the experiments was preregistered. The datasets and code generated during the current study are available in the Science Data Bank repository. <https://www.scidb.cn/s/nEJnQn>

Conflicts of interest The authors declare that there are no conflicts of interest.

References

- Allison, T., Puce, A., & McCarthy, G. (2000). Social perception from visual cues: Role of the STS region. *Trends in Cognitive Sciences*, 4(7), 267–278. [https://doi.org/10.1016/S1364-6613\(00\)01501-1](https://doi.org/10.1016/S1364-6613(00)01501-1)
- Ananyev, E., Penney, T. B., & Hsieh, P.-J. (2017). Separate requirements for detection and perceptual stability of motion in interocular suppression. *Scientific Reports*, 7(1), Article 7230. <https://doi.org/10.1038/s41598-017-07805-5>
- Brainard, D. H. (1997). The psychophysics toolbox. *Spatial Vision*, 10(4), 433–436. <https://doi.org/10.1163/156856897x00357>
- Cha, O., Son, G., Chong, S. C., Tovar, D. A., & Blake, R. (2019). Novel procedure for generating continuous flash suppression: Seurat meets Mondrian. *Journal of Vision*, 19(14), Article 1.
- Deen, B., Koldewyn, K., Kanwisher, N., & Saxe, R. (2015). Functional organization of social perception and cognition in the superior temporal sulcus. *Cerebral Cortex*, 25(11), 4596–4609. <https://doi.org/10.1093/cercor/bhv111>
- del Río, M., Greenlee, M. W., & Volberg, G. (2018). Neural dynamics of breaking continuous flash suppression. *NeuroImage*, 176, 277–289.
- Dong, X., Zhang, M., Dong, B., Jiang, Y., & Bao, M. (2022). Reward produces learning of a consciously inaccessible feature. *British Journal of Psychology*, 113(1), 49–67. <https://doi.org/10.1111/bjop.12518>
- Faivre, N., Berthet, V., & Kouider, S. (2014). Sustained invisibility through crowding and continuous flash suppression: A comparative review. *Frontiers in Psychology*, 5, Article 475. <https://doi.org/10.3389/fpsyg.2014.00475>
- Gayet, S., & Stein, T. (2017). Between-subject variability in the breaking continuous flash suppression paradigm: Potential causes, consequences, and solutions. *Frontiers in Psychology*, 8, Article 437.
- Gayet, S., Stigchel, S., & Paffen, C. (2013). Seeing is believing: Utilization of subliminal symbols requires a visible relevant context. *Attention, Perception & Psychophysics*, 76, 489–507. <https://doi.org/10.3758/s13414-013-0580-4>
- Gayet, S., Van der Stigchel, S., & Paffen, C. L. E. (2014). Breaking continuous flash suppression: Competing for consciousness on the pre-semantic battlefield. *Frontiers in Psychology*, 5, Article 460. <https://doi.org/10.3389/fpsyg.2014.00460>
- Giese, M. A., & Poggio, T. (2003). Neural mechanisms for the recognition of biological movements. *Nature Reviews Neuroscience*, 4(3), 179–192. <https://doi.org/10.1038/nrn1057>
- Goldstein, A., Rivlin, I., Goldstein, A., Pertzov, Y., & Hassin, R. R. (2020). Predictions from masked motion with and without obstacles. *PLoS One*, 15(11), Article e0239839. <https://doi.org/10.1371/journal.pone.0239839>
- Grossmann, T. (2015). The development of social brain functions in infancy. *Psychological Bulletin*, 141(6), 1266–1287. <https://doi.org/10.1037/bul0000002>
- Han, S., Lukaszewski, R., & Alais, D. (2019). Continuous flash suppression operates in local spatial zones: Effects of mask size and contrast. *Vision Research*, 154, 105–114. <https://doi.org/10.1016/j.visres.2018.11.006>
- Han, S., Lunghi, C., & Alais, D. (2016). The temporal frequency tuning of continuous flash suppression reveals peak suppression at very low frequencies. *Scientific Reports*, 6, Article 35723. <https://doi.org/10.1038/srep35723>
- Herrington, J. D., Nymberg, C., & Schultz, R. T. (2011). Biological motion task performance predicts superior temporal sulcus activity. *Brain and Cognition*, 77(3), 372–381. <https://doi.org/10.1016/j.bandc.2011.09.001>
- He, X., & Bao, M. (2024). Neuroimaging evidence of visual-vestibular interaction accounting for perceptual mislocalization induced by head rotation. *Neurophotonics*, 11(1), Article 015005. <https://doi.org/10.1117/1.NPh.11.1.015005>
- Hesselmann, G., & Malach, R. (2011). The link between fMRI-BOLD activation and perceptual awareness is “stream-invariant” in the human visual system. *Cerebral Cortex*, 21(12), 2829–2837. <https://doi.org/10.1093/cercor/bhr085>
- Hong, S. W., & Blake, R. (2009). Interocular suppression differentially affects achromatic and chromatic mechanisms. *Attention, Perception & Psychophysics*, 71, 403–411. <https://doi.org/10.3758/APP.71.2.403>
- Hou, X., Zhang, Z., Zhao, C., Duan, L., Gong, Y., Li, Z., & Zhu, C. (2021). NIRS-KIT: A MATLAB toolbox for both resting-state and task fNIRS data analysis. *Neurophotonics*, 8(1), Article 010802. <https://doi.org/10.1117/1.NPh.8.1.010802>
- Jastorff, J., & Orban, G. A. (2009). Human functional magnetic resonance imaging reveals separation and integration of shape and motion cues in biological motion processing. *Journal of*

- Neuroscience*, 29(22), 7315–7329. <https://doi.org/10.1523/JNEUROSCI.4870-08.2009>
- Jiang, Y., Costello, P., & He, S. (2007). Processing of invisible stimuli: Advantage of upright faces and recognizable words in overcoming interocular suppression. *Psychological Science*, 18(4), 349–355. <https://doi.org/10.1111/j.1467-9280.2007.01902.x>
- Jiang, Y., & Wang, L. (2011). Biological motion perception: The roles of global configuration and local motion. *Advances in Psychological Science*, 19(3), 301–311.
- Johansson, G. (1973). Visual perception of biological motion and a model for its analysis. *Perception & Psychophysics*, 14(2), 201–211. <https://doi.org/10.3758/BF03212378>
- Johansson, G. (1976). Spatio-temporal differentiation and integration in visual motion perception: An experimental and theoretical analysis of calculus-like functions in visual data processing. *Psychological Research*, 38(4), 379–393. <https://doi.org/10.1007/BF00309043>
- Kim, C.-Y., & Blake, R. (2005). Psychophysical magic: Rendering the visible ‘invisible.’ *Trends in Cognitive Sciences*, 9(8), 381–388. <https://doi.org/10.1016/j.tics.2005.06.012>
- Kim, C.-Y., Grossman, E. D., & Blake, R. (2013). Neural activity reflecting perceptual awareness of biologically relevant events. *Journal of the Korean Psychological Association: Cognitive and Biologica*, 25(2), 153–172. <https://doi.org/10.22172/cogbio.2013.25.2.002>
- Kim, J., Park, S., & Blake, R. (2011). Perception of biological motion in schizophrenia and healthy individuals: A behavioral and fMRI study. *PLoS One*, 6(5), Article e19971. <https://doi.org/10.1371/journal.pone.0019971>
- Lisboa, I. C., Miguel, H., Sampaio, A., Mouta, S., Santos, J. A., & Pereira, A. F. (2020). Right STS responses to biological motion in infancy – An fNIRS study using point-light walkers. *Neuropsychologia*, 149, Article 107668. <https://doi.org/10.1016/j.neuropsychologia.2020.107668>
- Lisboa, I. C., Queirós, S., Miguel, H., Sampaio, A., Santos, J. A., & Pereira, A. F. (2020). Infants’ cortical processing of biological motion configuration – A fnirs study. *Infant Behavior and Development*, 60, Article 101450. <https://doi.org/10.1016/j.infbeh.2020.101450>
- Liu, D., Wang, L., Wang, Y., & Jiang, Y. (2016). Conscious access to suppressed threatening information is modulated by working memory. *Psychological Science*, 27(11), 1419–1427. <https://doi.org/10.1177/0956797616660680>
- Liu, Y., Li, M., Zhang, X., Lu, Y., Gong, H., Yin, J., Chen, Z., Qian, L., Yang, Y., Andolina, I. M., Shipp, S., McLoughlin, N., Tang, S., & Wang, W. (2020). Hierarchical representation for chromatic processing across macaque V1, V2, and V4. *Neuron*, 108(3), 538–550.e5. <https://doi.org/10.1016/j.neuron.2020.07.037>
- Lloyd-Fox, S., Blasi, A., & Elwell, C. E. (2010). Illuminating the developing brain: The past, present and future of functional near-infrared spectroscopy. *Neuroscience and Biobehavioral Reviews*, 34(3), 269–284. <https://doi.org/10.1016/j.neubiorev.2009.07.008>
- Ludwig, K., Sterzer, P., Kathmann, N., & Hesselmann, G. (2016). Differential modulation of visual object processing in dorsal and ventral stream by stimulus visibility. *Cortex*, 83, 113–123. <https://doi.org/10.1016/j.cortex.2016.07.002>
- Mastropasqua, T., Tse, P. U., & Turatto, M. (2015). Learning of monocular information facilitates breakthrough to awareness during interocular suppression. *Attention, Perception, & Psychophysics*, 77(3), 790–803. <https://doi.org/10.3758/s13414-015-0839-z>
- Mei, G., Yuan, Q., Liu, G., Pan, Y., & Bao, M. (2018). Spontaneous recovery and time course of biological motion adaptation. *Vision Research*, 149, 40–46. <https://doi.org/10.1016/j.visres.2018.06.001>
- Moors, P., Wagemans, J., & de-Wit, L. (2014). Moving stimuli are less effectively masked using traditional continuous flash suppression (CFS) compared to a moving mondrian mask (MMM): A test case for feature-selective suppression and retinotopic adaptation. *PLoS One*, 9(5), Article e98298. <https://doi.org/10.1371/journal.pone.0098298>
- Mudrik, L., Breska, A., Lamy, D., & Deouell, L. (2011). Integration without awareness: Expanding the limits of unconscious processing. *Psychological Science*, 22(6), 764–770. <https://doi.org/10.1177/0956797611408736>
- Ogle, K. N., Mussey, F., & Avery De, H. P. (1949). Fixation disparity and the fusional processes in binocular single vision*. *American Journal of Ophthalmology*, 32(8), 1069–1087. [https://doi.org/10.1016/0002-9394\(49\)90649-2](https://doi.org/10.1016/0002-9394(49)90649-2)
- Paffen, C. L. E., Gayet, S., Heilbron, M., & Van Der Stigchel, S. (2018). Attention-based perceptual learning does not affect access to awareness. *Journal of Vision*, 18(3), Article 7. <https://doi.org/10.1167/18.3.7>
- Pavlova, M., & Sokolov, A. (2003). Prior knowledge about display inversion in biological motion perception. *Perception*, 32(8), 937–946. <https://doi.org/10.1068/p3428>
- Peelen, M. V., & Downing, P. E. (2007). The neural basis of visual body perception. *Nature Reviews Neuroscience*, 8(8), 636–648. <https://doi.org/10.1038/nrn2195>
- Pelphrey, K. A., Mitchell, T. V., McKeown, M. J., Goldstein, J., Allison, T., & McCarthy, G. (2003). Brain activity evoked by the perception of human walking: Controlling for meaningful coherent motion. *The Journal of Neuroscience*, 23(17), 6819–6825. <https://doi.org/10.1523/JNEUROSCI.23-17-06819.2003>
- Pelphrey, K. A., & Morris, J. P. (2006). Brain mechanisms for interpreting the actions of others from biological-motion cues. *Current Directions in Psychological Science*, 15(3), 136–140. <https://doi.org/10.1111/j.0963-7214.2006.00423.x>
- Peuskens, H., Vanrie, J., Verfaillie, K., & Orban, G. A. (2005). Specificity of regions processing biological motion. *European Journal of Neuroscience*, 21(10), 2864–2875. <https://doi.org/10.1111/j.1460-9568.2005.04106.x>
- Pinti, P., Tachtsidis, I., Hamilton, A., Hirsch, J., Aichelburg, C., Gilbert, S., & Burgess, P. W. (2020). The present and future use of functional near-infrared spectroscopy (fNIRS) for cognitive neuroscience. *Annals of the New York Academy of Sciences*, 1464(1), 5–29. <https://doi.org/10.1111/nyas.13948>
- Pournaghdali, A., & Schwartz, B. L. (2020). Continuous flash suppression: Known and unknowns. *Psychonomic Bulletin & Review*, 27(6), 1071–1103. <https://doi.org/10.3758/s13423-020-01771-2>
- Puce, A., & Perrett, D. (2003). Electrophysiology and brain imaging of biological motion. *Philosophical Transactions of the Royal Society of London. Series B, Biological Sciences*, 358(1431), 435–445. <https://doi.org/10.1098/rstb.2002.1221>
- Saygin, A. P., Wilson, S. M., Hagler, D. J., Bates, E., & Sereno, M. I. (2004). Point-light biological motion perception activates human premotor cortex. *Journal of Neuroscience*, 24(27), 6181–6188. <https://doi.org/10.1523/JNEUROSCI.0504-04.2004>
- Stein, T., Hebart, M., & Sterzer, P. (2011). Breaking continuous flash suppression: A new measure of unconscious processing during interocular suppression? *Frontiers in Human Neuroscience*, 5, Article 167.
- Stein, T., & Peelen, M. V. (2021). Dissociating conscious and unconscious influences on visual detection effects. *Nature Human Behaviour*, 5(5), 612–624. <https://doi.org/10.1038/s41562-020-01004-5>
- Stein, T., & Sterzer, P. (2014). Unconscious processing under interocular suppression: Getting the right measure. *Frontiers in Psychology*, 5, Article 387. <https://doi.org/10.3389/fpsyg.2014.00387>
- Strangman, G., Culver, J. P., Thompson, J. H., & Boas, D. A. (2002). A quantitative comparison of simultaneous BOLD fMRI and NIRS recordings during functional brain activation. *NeuroImage*, 17(2), 719–731. <https://doi.org/10.1006/nimg.2002.1227>

- Sun, Y., Stein, T., Liu, W., Ding, X., & Nie, Q.-Y. (2017). Biphasic attentional orienting triggered by invisible social signals. *Cognition*, 168, 129–139. <https://doi.org/10.1016/j.cognition.2017.06.020>
- Sun, Y., Wang, X., Huang, Y., Ji, H., & Ding, X. (2022). Biological motion gains preferential access to awareness during continuous flash suppression: Local biological motion matters. *Journal of Experimental Psychology: General*, 151(2), 309–320. <https://doi.org/10.1037/xge0001078>
- Timmermans, B., & Cleeremans, A. (2015). How can we measure awareness? An overview of current methods. In M. Overgaard (Ed.), *Behavioral Methods in Consciousness Research* (pp. 21–46). Oxford University Press.
- Troje, N. (2013). What Is Biological Motion? Definition, Stimuli, and Paradigms. In M. D. Rutherford & V. A. Kuhlmeier (Eds.), *Social Perception: Detection and Interpretation of Animacy, Agency, and Intention* (pp. 13–36). MIT Press. <https://doi.org/10.7551/mitpress/9780262019279.003.0002>
- Troje, N. F., & Westhoff, C. (2006). The inversion effect in biological motion perception: Evidence for a “life detector”? *Current Biology*, 16(8), 821–824. <https://doi.org/10.1016/j.cub.2006.03.022>
- Tsuchiya, N., & Koch, C. (2005). Continuous flash suppression reduces negative afterimages. *Nature Neuroscience*, 8(8), 1096–1101. <https://doi.org/10.1038/nn1500>
- Tsuchiya, N., Koch, C., Gilroy, L. A., & Blake, R. (2006). Depth of interocular suppression associated with continuous flash suppression, flash suppression, and binocular rivalry. *Journal of Vision*, 6(10), Article 6. <https://doi.org/10.1167/6.10.6>
- van Boxtel, J. J. A., & Lu, H. (2013). A biological motion toolbox for reading, displaying, and manipulating motion capture data in research settings. *Journal of Vision*, 13(12), Article 7. <https://doi.org/10.1167/13.12.7>
- Vermeiren, A., & Cleeremans, A. (2012). The validity of d' measures. *PLoS One*, 7(2), Article e31595. <https://doi.org/10.1371/journal.pone.0031595>
- Wang, G., Alais, D., Blake, R., & Han, S. (2022). CFS-crafter: An open-source tool for creating and analyzing images for continuous flash suppression experiments. *Behavior Research Methods*, 55, 2004–2020. <https://doi.org/10.3758/s13428-022-01903-7>
- Wang, R., Lu, X., & Jiang, Y. (2023). Distributed and hierarchical neural encoding of multidimensional biological motion attributes in the human brain. *Cerebral Cortex*, 33(13), 8510–8522. <https://doi.org/10.1093/cercor/bhad136>
- Wu, B., Li, J., He, H., Hou, Y., Jia, Y., & Feng, S. (2019). Categorical perception of color can be instantly influenced by color vision fatigue and semantic satiation. *Acta Psychologica Sinica*, 51(2), 196–206. <https://doi.org/10.3724/SP.J.1041.2019.00196>
- Xiao, X., Yu, X., Zhang, Z., Zhao, Y., Jiang, Y., Li, Z., Yang, Y., & Zhu, C. (2018). Transcranial brain atlas. *Science Advances*, 4(9), Article eaar6904. <https://doi.org/10.1126/sciadv.aar6904>
- Yang, E., Brascamp, J., Kang, M.-S., & Blake, R. (2014). On the use of continuous flash suppression for the study of visual processing outside of awareness. *Frontiers in Psychology*, 5, Article 724. <https://doi.org/10.3389/fpsyg.2014.00724>
- Zhao, J., & Bao, M. (2022). A method for studying unconscious motion processing based on the camouflage principle. *Acta Psychologica Sinica*, 54(7), 725–735. <https://doi.org/10.3724/SP.J.1041.2022.00725>

Publisher's Note Springer Nature remains neutral with regard to jurisdictional claims in published maps and institutional affiliations.

Springer Nature or its licensor (e.g. a society or other partner) holds exclusive rights to this article under a publishing agreement with the author(s) or other rightsholder(s); author self-archiving of the accepted manuscript version of this article is solely governed by the terms of such publishing agreement and applicable law.